



**Emerging investigator series: Radium Accumulation in
Carbonate River Sediments at Oil and Gas Produced Water
Discharges: Implications for Beneficial Use as Disposal
Management**

Journal:	<i>Environmental Science: Processes & Impacts</i>
Manuscript ID	EM-ART-07-2018-000336.R2
Article Type:	Paper
Date Submitted by the Author:	20-Nov-2018
Complete List of Authors:	<p>McDevitt, Bonnie; The Pennsylvania State University , Civil and Environmental Engineering McLaughlin, Molly; Colorado State University, Civil and Environmental Engineering Cravotta, Charles; US Geological Survey Water Science Center Pennsylvania Ajemigbitse, Moses; The Pennsylvania State University , Civil and Environmental Engineering Van Sice, Katherine; The Pennsylvania State University , Civil and Environmental Engineering Blotevogel, Jens; Colorado State University, Civil and Environmental Engineering Borch, Thomas; Colorado State University, Soil and Crop Sciences; Colorado State University, Chemistry; Colorado State University, Civil and Environmental Engineering Warner, Nathaniel; The Pennsylvania State University , Civil and Environmental Engineering</p>

1
2
3 **Emerging investigator series: Radium Accumulation in Carbonate River Sediments at Oil and Gas**
4 **Produced Water Discharges: Implications for Beneficial Use as Disposal Management**
5

6 Bonnie McDevitt^a, Molly McLaughlin^b, Charles A. Cravotta III^c, Moses A. Ajemigbitse^a, Katherine J. Van
7 Sice^a, Jens Blotevogel^b, Thomas Borch^{bde}, Nathaniel R. Warner^{a1}
8
9

10 ^a Department of Civil and Environmental Engineering, The Pennsylvania State University, University Park,
11 PA 16802, United States
12

13 ^b Department of Civil and Environmental Engineering, Colorado State University, 1320 Campus Delivery,
14 Fort Collins, Colorado 80523, United States
15

16 ^c U.S. Geological Survey, Pennsylvania Water Science Center, 215 Limekiln Road, New Cumberland, PA
17 17070, United States
18

19 ^d Department of Soil and Crop Sciences, Colorado State University, 1170 Campus Delivery, Fort Collins,
20 Colorado 80523, United States
21

22 ^e Department of Chemistry, Colorado State University, 1872 Campus Delivery, Fort Collins, Colorado
23 80523, United States
24

25 ¹ Corresponding author: nrw6@psu.edu
26
27

28 **Abstract**
29

30 In the western U.S., produced water from oil and gas wells discharged to surface water augments
31 downstream supplies used for irrigation and livestock watering. Here we investigate six permitted
32 discharges on three neighboring tributary systems in Wyoming. During 2013-16, we evaluated radium
33 activities of the permitted discharges and the potential for radium accumulation in associated stream
34 sediments. Radium activities of the sediments at the points of discharge ranged from approximately
35 200-3600 Bq/kg with elevated activities above the background of 74 Bq/kg over 30 km downstream of
36 one permitted discharge. Sediment as deep as 30 cm near the point of discharge had radium activities
37 elevated above background. X-ray diffraction and targeted sequential extraction of radium in sediments
38 indicate that radium is likely coprecipitated with carbonate and, to a lesser extent, sulfate minerals.
39 PHREEQC modeling predicts radium coprecipitation with aragonite and barite, but over-estimates the
40 latter compared to observations of downstream sediment, where carbonate predominates. Mass-
41 balance calculations indicate over 3 billion Bq of radium activity (²²⁶Ra+²²⁸Ra) is discharged each year
42 from five of the discharges, combined, with only 5 percent of the annual load retained in stream
43 sediments within 100m of the effluent discharges; the remaining 95 percent of the radium is
44 transported farther downstream as sediment-associated and aqueous species.
45
46
47
48
49
50
51
52
53
54
55
56
57
58
59
60

Environmental Significance Statement

In western U.S. states, billions of liters of oil and gas wastewater are discharged to frequently dry, ephemeral stream beds for beneficial reuse. Elevated sediment radium accumulations at points of discharge were observed though effluents contained relatively low dissolved radium concentrations. Because receiving streams offer little dilution benefit for elevated TDS effluent concentrations, observed coprecipitation of radium with carbonate, and to less extent, sulfate minerals, remain a secondary contamination source after effluent discharges cease. As observed with sediment leaching experiments, storm events could resuspend fine-grained sediment particles to the water column for transport downstream, or acidic rain and solubility changes could alter saturation of carbonate minerals, specifically, allowing radium to remobilize as aqueous species that could be bioavailable.

Introduction

Eighty percent of the United States' produced water brought to the surface during oil and gas (O&G) extraction processes is generated in states west of the 98th meridian.¹ In these western states, produced waters are frequently discharged to surface waters in the O&G fields through the National Pollutant Discharge Elimination System (NPDES) and, according to 40 CFR § 435 Subpart E, permitted for beneficial reuse downstream for irrigation, livestock watering, and wildlife propagation. While there remain effluent limits in place for pollutants, the regulations for consistent self-reporting Discharge Monitoring Reports (DMR) are relatively limited and variable by state and discharge. In arid and semi-arid regions, regional NPDES discharges may offer an additional, and in some cases substantial, water resource that can aid in boosting local agricultural economies; however, more research related to human health directly associated with produced water disposal in western regions is needed as ecological impacts to *Daphnia magna* and rainbow trout have been observed.²⁻⁴ In these older O&G fields, with low O&G to produced water ratios, production would likely be economically unviable if produced waters required treatment beyond basic oil-water-gas-separation and settling before disposal to ephemeral stream beds.

Depending on geologic formation characteristics, produced waters can be highly saline solutions, causing concern for their discharges to surface waters from centralized waste treatment facilities (CWTs) as exhibited in numerous studies in Pennsylvania and the Eastern US with some observed impacts more than 20 km downstream of the discharge.⁵⁻¹³ Produced water discharges increase concentrations of

1
2
3 dissolved naturally occurring radioactive material (NORM), chloride, boron, fluoride, organic
4 contaminants, and trace metals such as arsenic.¹⁴⁻¹⁶

5
6
7 Radium, a highly soluble component of NORM found in naturally low concentrations in the environment,
8 is a radioactive alkaline earth metal exhibiting similar environmental behavior to calcium, barium,
9 strontium, and magnesium (Ca, Ba, Sr and Mg) that is known to cause lymphoma, bone cancer, and
10 leukemia at higher concentrations due to the uptake of the radium ion into animal bones and calcium-
11 rich tissues where it then decays.^{17,18} Radon, a short-lived daughter product of radium decay, is a
12 radioactive gas known to cause lung cancer.¹⁹ Radium-226 ($t_{1/2}$ = 1600 years) and radium-228 ($t_{1/2}$ = 5.75
13 years) (^{226}Ra + ^{228}Ra) are the two most persistent radioisotopes of radium, respectively sourced from
14 parent rock material uranium-238 and parent rock material thorium-232. Most states and the EPA
15 regulate ^{226}Ra for O&G produced water disposal to surface water at 2.22 Bq/L (60 pCi/L), though the
16 drinking water standard is set much lower at 0.185 Bq/L (5 pCi/L) for combined ^{226}Ra + ^{228}Ra .^{20,21}
17 Compared to the well-characterized, high salinity Appalachian Basin produced waters with median Total
18 Dissolved Solids (TDS) concentrations of 250,000 mg/L and median ^{226}Ra concentrations of around 111
19 Bq/L, median TDS concentrations in Wyoming formations, mined from the USGS Produced Water
20 Database (<https://energy.usgs.gov/>), range from 4,000 to 10,000 mg/L with a much lower reported ^{226}Ra
21 concentration of 3.14 Bq/L in the Niobrara formation produced water.^{15,22}

22
23
24 Once discharged, radium often associates with suspended particles and other precipitating ions and
25 accumulates in streambed sediments where the action level according to 40 CFR 192 for ^{226}Ra in the top
26 15 cm of surface soils in inactive uranium and thorium processing sites should not exceed 185 Bq/kg (5
27 pCi/g) above background concentrations and not exceed 555 Bq/kg (15 pCi/g) above background in any
28 15 cm layer below the surface layer in any 100 square meter area (www.ecfr.gov). Combined ^{226}Ra +
29 ^{228}Ra accumulation in sediments 200 times background were noted at the discharge of a brine treatment
30 facility disposing treated produced water with a mean ^{226}Ra concentration of 1.97 Bq/L to a stream in
31 Pennsylvania with observed radium concentrations 1.5 times background up to 31 km downstream from
32 the discharge in reservoir surface sediments and sediment cores 3 years later.^{5,23} Additional facilities in
33 Pennsylvania also showed elevated radium activities at the discharges with mean radium values in
34 sediments from 740 to 7400 Bq/kg, with much of the activity attributed to conventional O&G brines
35 typically produced from the Appalachian Basin.¹³ In a 2015 O&G pipeline fluid spill in Williston Basin,
36 North Dakota sediments contained combined ^{226}Ra + ^{228}Ra , which is 15-100 times background,
37 depending on the study, though the pipeline fluid concentration was relatively low around 0.33 Bq/L

1
2
3 indicating high potential for radium to continually impact ecosystems long-term as a secondary
4 contaminant source through transport of radium-enriched sediments and subsequent release into
5 aqueous phase.^{24,25}
6
7

8
9 The mobility, bioavailability, and toxicity of radium in the aqueous environment depends on its phase as
10 an aqueous species Ra^{2+} , RaOH^+ , RaCl^+ , RaCO_3^0 , or RaSO_4^0 ; sorbed to clays, organic matter, and ferric and
11 manganese oxides; or co-precipitated into sulfate and carbonate minerals.²⁶ Radium preferentially co-
12 precipitates with sulfate and barium or strontium when supersaturated to form radiobarite $(\text{Ba,Ra})\text{SO}_4$
13 and radiocelstite $(\text{Sr,Ra})\text{SO}_4$ compared to co-precipitation with supersaturated carbonate minerals.^{27,26}
14 Menzie et al. (2008) demonstrated the low risk for bioaccumulation and toxicity of radiobarite due to its
15 insolubility.²⁷ However, once radium in sulfate minerals accumulates with easily transported fine-
16 grained sediments and mobilizes to areas with lower concentrations and anoxic conditions, reduction of
17 sulfate minerals by sulfate-reducing bacteria can release the Ra, Sr and Ba back into solution posing a
18 potential risk for bioavailability of the radium.²⁸⁻³⁰ In the Eastern US some produced waters were
19 discharged to streams and the ultimate fate of the radium is unclear.³¹ Radium sequestration by
20 partitioning into sulfate solid solutions involving barite (BaSO_4) and celestite (SrSO_4) is widely reported;
21 however, incorporation of radium into calcium carbonate (CaCO_3), strontianite (SrCO_3), witherite
22 (BaCO_3), and other carbonate phases is less well established.³²⁻⁴⁶ Because cations with crystal ionic radii
23 larger than Ca^{2+} can fit well in the orthorhombic structure, aragonite may take up significant amounts of
24 Sr^{2+} , Pb^{2+} , Ba^{2+} and, presumably, Ra^{2+} , compared to rhombohedral calcite, which has low potential for
25 equilibrium partitioning of Sr and Ba.^{44,45,47-49} Additional carbonate phases including dolomite, ankerite,
26 magnesite, and siderite exhibit potential for adsorption of low concentrations of Ra^{2+} and Ba^{2+} .⁵⁰
27 Carbonates generally dissolve more readily than celestite and barite suggesting potential for radium re-
28 mobilization to the water column in response to episodic dilution and acidification.⁵¹
29
30
31
32
33
34
35
36
37
38
39
40
41
42

43 To the authors' knowledge this study is the first temporal and spatial characterization of produced water
44 discharges for beneficial reuse and sediment radium accumulation in the Western US. The study aims to
45 (1) characterize sediment radium accumulation with distance from six discharge sites compared to a
46 background reference site, (2) observe changes in radium concentration with depth in a stream-
47 sediment profile, (3) investigate the adsorption and/or co-precipitation mechanism(s) controlling radium
48 accumulation in sediments, (4) develop a model that includes solid solution radium minerals to predict
49 the fate and transport of anthropogenic radium, and (5) provide recommendations regarding NPDES 40
50 CFR § 435 Subpart E based on radium bioavailability potential.
51
52
53
54
55
56
57
58
59
60

Materials and Methods

Site Description

Wyoming generates the fourth largest volume of produced water in the United States after Texas, California and Oklahoma with 2.18 billion barrels per year as of 2012 and practices beneficial use of produced water for disposal to surface water.⁵² This investigation focused on a large river basin in Wyoming that contains two major perennial rivers (B and C) and a naturally ephemeral tributary (A) (Figure 1). The precise locations are not disclosed in accordance with access agreements with private land owners. The studied stream systems (A, B and C) include ephemeral tributary segments that drain arid plains where cattle and other wildlife range; the NPDES produced water discharges constitute much of the streamflow in the tributaries. Generally, the stream channels are incised through Tertiary and Quaternary alluvium colluvium, and fan deposits, which contain gypsum, carbonate, and silicate sediments derived from Cretaceous bedrock in headwaters. . Background water and sediment samples were collected from background site UDB-1.0 upstream of all River B NPDES facilities; however, upstream sediment and water samples were not collected from Tributary A and River C NPDES facilities because the NPDES facilities in large O&G fields were the source of the streams. A reference tributary without known O&G development was also sampled west of Tributary A and was mostly dry during sampling events. More detailed site information is included in the Supplemental Information (ESI).

In the study area, O&G extraction occurred through wells drilled vertically into reservoirs that have been hydraulically fractured to increase permeability and productivity. The five major reservoirs of oil and gas, from youngest (Cretaceous) to oldest (Pennsylvanian), are the Mesaverde Formation, Nugget Formation, Chugwater Formation, Phosphoria Formation, and Tensleep Sandstone. All NPDES facilities treated produced water similarly with basic oil-gas-water separation (pressure chamber, three phase separator, and heater treater) and a series of settling and skim tank(s)/pond(s) where oil in excess of 1.3 cm depth on the water surface at one facility was removed by vacuum once every two months, before discharge to the otherwise dry, ephemeral stream bed.

Water and Sediment Sample Collection

Water samples were collected during 10 sampling events between 2013 and 2016 at 28 sites. Sampling occurred in May and November 2013, May, July and October 2014, July and October 2015 and June, August and October 2016. Streamflows in the larger Tributary A and Rivers B and C, determined from USGS stream gauges, indicated relatively constant flows during sampling events except for one potential

1
2
3 outlier with peak flows during the June 2016 sampling event likely due to heavy snowmelt not captured
4 during other sampling years; more detailed sampling information is included in the Supplemental
5 Information (ESI). Specific conductance, pH, temperature, and dissolved oxygen were measured in the
6 field at each location using a Hydrolab field meter. Water samples were field filtered with 0.45 μ m pore
7 size cellulose acetate membranes for major anion analysis and then preserved with nitric acid (HNO₃) to
8 pH less than 2 for major cation and trace metal analysis. All samples were stored at 4°C in the laboratory
9 before analysis.

10
11
12
13
14
15
16 Grab sediment samples were collected in triplicate from the upper 5 cm of sediment surface during 2
17 sampling events in August and October 2016. Five 4-inch diameter sediment push-tube cores of varying
18 depths were collected in October 2016 directly at discharge facility DC-1 (34 cm) and 100 m downstream
19 (22 cm), 1 km downstream from discharge facility DB-2.0 (22 cm), and downstream from discharge
20 facilities DA-2 (24 cm) and DA-3 (16 cm). Cores were frozen in the laboratory until analysis. Both grab
21 sediment samples and sediment cores were collected from the sides of the stream channels, avoiding
22 large boulders and rocks, from sediments at the water surface level. If a stream channel meandered,
23 sediments were collected from the point bar side of the bend to capture sediment accumulation.

24 25 26 27 28 29 30 *Water Sample Analysis*

31
32
33 Filtered, acidified water samples were analyzed for major cations by inductively coupled plasma atomic
34 emission spectroscopy (ICP-AES) and ICP mass spectrometry (ICP-MS) for trace metals. Filtered, non-
35 acidified samples were analyzed for major anions by ion chromatography (IC). Samples with major
36 anion/cation charge balances greater than 15% difference were not included in the statistical analysis.
37 Four samples out of 247 total samples (less than 2% of samples) did not meet this criterion, two of
38 which were collected at the reference sample site due to a lack of sufficient available water sample for
39 anion IC analysis.

40
41
42
43
44
45 Dissolved radium-226 activities were analyzed by a modified EPA Eichrom method where radium was
46 coprecipitated with barium sulfate and then analyzed via alpha spectrometry.⁵³ Dissolved radium-228
47 was measured using a modified EPA RA-05 method with precipitation and analysis via beta
48 spectrometry.⁵⁴

49 50 51 52 53 *Sediment Sample and Core Processing*

1
2
3 Sediment samples were dried, ground with mortar and pestle, and sieved to 1.18 mm size fraction to
4 exclude large rocks and organic material. Sediment was then packed into 20-mL high-density
5 polyethylene vials, and sealed with tape to prevent the escape of ^{222}Rn for at least 21 days to allow for
6 establishment of secular equilibrium of ^{226}Ra daughter products (^{214}Pb and ^{214}Bi). Samples were then
7 measured on a Canberra small anode germanium gamma ray spectrometer (SAGe) detector located in
8 the SALTS lab at The Pennsylvania State University. ^{226}Ra activity was reported as the average activity of
9 351.93, 295.22, and 609.31 keV peaks and ^{228}Ra was measured using the 911.20 keV peak (^{228}Ac).
10 Samples were measured to counting errors less than 5% per peak and background counts were
11 subtracted. A uranium ore tailing standard (UTS-2) from Canadian Certified Reference Material Project
12 with certified activities was used as a calibration standard for detector efficiency calculations in the
13 same vial geometry as samples (<http://www.nrcan.gc.ca/mining-materials/>). The standard was
14 prepared, sealed, and measured in the same manner as the samples.
15
16
17
18
19
20
21
22
23

24 Sediment cores were extruded from the casing and sectioned into 4 cm intervals prior to processing.
25 Porewaters were extracted by centrifuge and pH and conductivity were measured immediately.
26 Porewaters were then filtered and preserved to pH less than 2 with HNO_3 for cation analysis by ICP-AES.
27 Sediments were then processed similarly to grab sediments in triplicate for radium measurement. ^{228}Ra
28 measurements were adjusted for the decay since collection by multiplying by the decay constant and
29 adding to the measured value. Additionally, ^{210}Pb was measured through 47 keV and ^{228}Th was
30 measured through the ^{212}Pb peak (239 keV) in order to apply age dating techniques.⁵⁵
31
32
33
34
35
36

37 *Sediment Characterization*

38
39
40 Selected grab sediment samples from the DC-1 and DB-2.0 produced water streams (DC-1, DC-2, DC-3,
41 C1, C3, Reference site, DB-2.0, DB-2.1 and DB-2.2) (n=9) were grain-sized by sieve on a shaker for 15
42 minutes into three categories: coarse sand (>300 μm), fine sand (<300 μm and >45 μm), and silt+clay
43 (<45 μm). Grain-sized samples were measured on the SAGe for radium measurement and then analyzed
44 on a PANalytical Empyrean X-Ray Diffractometer (XRD) and Jade software in the Materials
45 Characterization Lab (MCL) at The Pennsylvania State University for quantitative mineralogy with
46 enhanced resolution. Mineralogy of the total sample was combined using the three known grain-sized
47 masses.
48
49
50
51
52

53 A four step sequential leaching procedure modified from Phan et al. (2015) and Stewart et al. (2015) was
54 performed on the same grab sediments analyzed for mineralogy (n=9) with a solution to sediment ratio
55
56
57
58
59
60

1
2
3
4 of 20:1 to facilitate detection limits of major cations in the leachates.^{56,57} The operationally defined
5 procedure used to determine radium speciation was as follows:
6
7

- 8 1. Water soluble fraction targeted using ultra-pure distilled water and shaken for 24 hours
- 9 2. Exchangeable cation fraction targeted using 1M ammonium acetate buffered to pH 8 with
10 ammonium hydroxide to prevent carbonate dissolution and shaken for 12 hours
- 11 3. Carbonate fraction dissolved using 8% ultra-pure glacial acetic acid (pH=2.3) and shaken for
12 12 hours
- 13 4. Oxide fraction (i.e. iron and manganese oxides) targeted using 0.1M ultra-pure hydrochloric
14 acid and shaken for 12 hours
15
16
17
18
19

20 After each leaching step, samples were centrifuged at 10,000 RPM for 10 minutes, leachates were
21 filtered through 0.45 μm pore-size nylon filters, and remaining residues were freeze-dried and analyzed
22 on the SAGe for radium activities (adjusted for measurement 1.75 years after sampling). Because leach
23 residues were not incubated for at least 21 days, ^{226}Ra activities were quantified by direct measurement
24 at 186 keV following peak deconvolution to correct for ^{235}U interference. After steps 2-4, solid residue
25 was rinsed three times with ultra-pure distilled water, shaken, centrifuged, and filtered to ensure
26 complete removal of targeted species and the rinse water was recombined with original leachate
27 removed. Leachates were analyzed immediately for pH and preserved with HNO_3 for major cation
28 analysis by ICP-AES. Two leach step 4 residues (DC-1 and DB-2.0) were analyzed by Scanning Electron
29 Microscopy (SEM) and Energy Dispersive X-ray Spectroscopy (EDS) using a FEI Quanta 250
30 Environmental SEM and Aztec software to observe remaining element associations.
31
32
33
34
35
36
37

38 *Geochemical Modelling of Radium*

39

40 The PHREEQC 3.4.0 aqueous geochemical program was used to compute aqueous and surface
41 speciation and potential for selected minerals to precipitate from the NPDES effluents and associated
42 stream waters.⁵⁸ PHREEQC was used with the "phreeqc.dat" data base augmented with
43 thermodynamic data for additional solids from the "wateq4f.dat" data base and for radium species
44 and phases from "sit.dat," both provided with PHREEQC 3.4.0.^{59,60} The two radium phases considered
45 relevant for this study, RaCO_3 and RaSO_4 , which are included in sit.dat, utilize thermodynamic
46 equilibrium constants from Langmuir and Riese (1985).⁶¹ In addition to direct output of the mineral
47 saturation index (SI) values for pure phases, SI values for possible carbonate or sulfate solid-solution
48 series containing radium were estimated as the log of the sum of saturation ratios ($\text{SR} = \text{IAP}/\text{K}$) of the
49 components in the solid solution. For example, SI for $(\text{Ca,Ra})\text{CO}_3$ solid solution was computed as
50
51
52
53
54
55
56
57
58
59
60

1
2
3 $\log((a_{\text{Ra}^{2+}} \cdot a_{\text{CO}_3^{2-}}) / K_{\text{RaCO}_3} + (a_{\text{Ca}^{2+}} \cdot a_{\text{CO}_3^{2-}}) / K_{\text{Aragonite}})$, where “a” denotes activity of the ion and K is the
4 solubility constant. Aqueous speciation results were also used to estimate the ionic contributions to
5 the specific conductance (SC) in accordance with methods of McCleskey et al. (2012).⁶² Example
6 PHREEQC codes used for the above simulations and selected graphical results are included in the
7 Supplemental Information (ESI).
8
9

10
11
12
13 Although the chemical precipitation of ternary solid solutions such as (Ba, Sr, Ra)SO₄ may take place in
14 highly saturated systems and can be modeled using PHREEQC, Zhang et al. (2014) reported that the
15 removal of radium by interaction with barite or (Sr, Ba)SO₄ were similar, and Rosenberg et al. (2018)
16 reported the removal of radium during seawater evaporation could be modeled adequately by
17 chemical precipitation of a binary solid solution of Ra_xBa_{1-x}SO₄.^{32,42,43,63,64} Furthermore, sampled stream
18 water and sediment cores collected for this evaluation were not in direct contact and, therefore, do
19 not represent equilibrium distributions for the elements. Thus, models considering ternary solid-
20 solutions could not be constrained and were deemed unnecessary for the current evaluation of
21 predominant radium sequestration mechanisms downstream of effluents. Geochemical models
22 presented herewith evaluated potential for the incorporation of Ra²⁺ by solid solutions and its
23 adsorption by hydrous ferric oxide (HFO) and hydrous manganese oxide (HMO), but did not consider
24 the additional potential for its adsorption on carbonate surfaces, which could be important in a system
25 with actively accumulating carbonate minerals.⁵⁰
26
27
28
29
30
31
32
33
34
35

36 37 **Results and Discussion**

38 39 *Chemistry of Produced Water Discharges, Stream Water, and Stream Sediment*

40
41
42 Produced water discharge sites generally had higher than background water temperatures, lower than
43 background dissolved oxygen concentrations, and elevated hydrogen sulfide gas levels prompting the
44 use of personal monitors at some sites. Table S1 provides the averages of the major anions and cations
45 of interest with regard to radium coprecipitation, water types, and average field parameters for sites.
46 Generally, TDS concentrations in the produced water discharges were consistent with reported data in
47 the USGS Produced Water Database for Wyoming formations in that they were brackish-type waters
48 and dominated by sodium-sulfate or calcium-sulfate water types, rather than sodium chloride as
49 reported in the Eastern US Appalachian Basin brines.⁶⁵ Background river water types were dominated
50 more by calcium-bicarbonate type waters.
51
52
53
54
55
56
57
58
59
60

1
2
3 TDS, SC, and corresponding solute concentrations for the NPDES effluents and downstream waters
4 collected during 2013-16 indicate two general hydrologic processes in the study area: (1) mixing of
5 relatively elevated TDS effluents with lower TDS stream water, and (2) evaporation of waters along
6 produced water streams until additional mixing with inflows of lower TDS river waters. Downstream
7 trends in solute concentrations and pH (Table S1 and Figure S1) are affected by these major processes
8 plus equilibration to atmospheric conditions, mineral precipitation, and other geochemical reactions, as
9 explained below in the geochemical modeling. Linear regressions (R version 0.99.486) of dissolved
10 concentrations versus dissolved oxygen concentrations measured along the DC-1 produced water
11 stream indicated that as dissolved oxygen concentrations increased (a surrogate for distance), dissolved
12 SO_4 concentrations increased ($R^2=0.508$, $p<0.01$), dissolved Ba concentrations decreased ($R^2=0.65$,
13 $p<0.01$) and dissolved $^{226}\text{Ra}+^{228}\text{Ra}$ decreased ($R^2=0.63$, $p<0.01$) while dissolved Ca and Sr decreases were
14 not significant.

23
24 When compared by sample site, Wilcoxon rank sum statistical tests with conservative Bonferroni
25 corrections indicated River B and C stream system discharges (DC-1, DB-1.0, DB-2.0 and DB-4.0) had
26 significantly higher values for TDS and all major anions and cations ($p<0.05$) compared to the
27 downstream river sites (C1, C2, C3, B1, B2, B3). Uniquely, Tributary A sample sites (A1, A2, A3 and A4)
28 had significantly higher concentrations for TDS, chloride (Cl), sulfate (SO_4), and sodium (Na) compared to
29 the discharge sites ($p<0.05$) (DA-1, DA-2, and DA-3). Increased major ion concentrations downstream of
30 the NPDES discharge sites likely result from evaporation and oxidation of hydrogen sulfide downstream.

31
32 Dissolved effluent ^{226}Ra values measured during this study were greater than background activities but
33 lower than the 2.22 Bq/L (60 pCi/L) effluent limit (Table 1), similar to values reported for effluent from
34 facilities in Pennsylvania that treat O&G wastewater.³¹ However, facility DB-2.0, with one measured
35 sample from October 2016, had the highest measured ^{226}Ra value of 1.24 Bq/L, 62 times the average
36 activity measured at the Reference site, and a $^{226}\text{Ra}+^{228}\text{Ra}$ measured value of 2.12 Bq/L, 106 times the
37 average measured at the Reference site. These activities were also 212 times the average background
38 water activity of $^{226}\text{Ra}+^{228}\text{Ra}$ collected from site UDB-1.0 upstream of all discharges. From DB-2.0
39 permits, the average $^{226}\text{Ra}+^{228}\text{Ra}$ discharged was 0.81 Bq/L and maximum value was 1.41 Bq/L. Discharge
40 DC-1 had water $^{226}\text{Ra}+^{228}\text{Ra}$ activities 21.5 times higher compared to the Reference site and site DA-3
41 had activities 19.5 times Reference.

42
43 Though mean dissolved ^{226}Ra and dissolved $^{226}\text{Ra}+^{228}\text{Ra}$ activities were greater at all discharge sites in
44 each stream system compared to the river sites and background Reference site, activities decreased
45
46
47
48
49
50
51
52
53

1
2
3 within a relatively short distance downstream and before confluence points with the larger rivers. For
4 example, the DC-1 produced water stream decreased to around 2 times background water activities of
5 $^{226}\text{Ra}+^{228}\text{Ra}$ measured at the Reference site within about 15 km downstream of the discharge and 1.2
6
7 times background approximately 32 km downstream beyond which the produced water stream
8
9 frequently dried before reaching and mixing with River C. Within 1 km downstream of DB-2.0, dissolved
10
11 $^{226}\text{Ra}+^{228}\text{Ra}$ activities decreased substantially from 212 times background immediately below the
12
13 discharge pipe to 70 times; however, activities more than 2 km downstream were still 42 times
14
15 Reference.

16
17 While site DB-2.0 discharged produced water with the highest measured dissolved ^{226}Ra and $^{226}\text{Ra}+^{228}\text{Ra}$
18
19 value in this study, the average reported discharge volume (3.6 L/s) was a magnitude lower than the
20
21 facility near DA-3 and two magnitudes lower than DC-1, and facilities near DA-1 and DA-2 (Table S2).
22
23 When applying the reported average discharge volumes and measured average $^{226}\text{Ra}+^{228}\text{Ra}$ activities
24
25 from each facility or just downstream, total radium loadings to streams remain hundreds of millions of
26
27 Bq of activity per year from each NPDES facility. Assuming all discharged radium was sediment
28
29 associated with a constant porosity on a dry weight basis and homogeneously distributed, a basic mass
30
31 balance calculation assuming a control volume of 30m^3 (1m wide stream, 0.30m deep, and 100m long)
32
33 and sediment density of 1.2 g/cm^3 using the DC-1 average discharge volume (52.1 L/s) and measured
34
35 average total dissolved radium (0.43 Bq/L), leads to sediment activity of approximately 19,400 Bq/kg –
36
37 much more than measured sediment activities of around 925 Bq/kg. According to this calculation,
38
39 observed values indicated that less than 5% of annually discharged effluent radium remains in sediment
40
41 within 100m of the discharge, though the actual percent is most likely much lower due to many years of
42
43 Ra loading not considered here. Thus, the radium is either transported with surface or groundwater in
44
45 either dissolved or particle associated form which could have implications for both human and
46
47 ecological health depending on its ultimate fate downstream as sorbed, precipitated, or aqueous
48
49 species.

50
51 Sediment radium activities followed similar trends to the dissolved $^{226}\text{Ra}+^{228}\text{Ra}$ activities in the water
52
53 with much larger activities measured at discharge facilities as compared to background and
54
55 river/tributary sites and decreasing activities with increasing distance downstream (Table 1 and Figure
56
57 2A, 3A, 4A). Ratios of $^{228}\text{Ra}/^{226}\text{Ra}$ versus distance from the discharge were also plotted (Figure 2B, 3B,
58
59 4B). Discharge sites DA-2 and DA-3 had significantly higher $^{226}\text{Ra}+^{228}\text{Ra}$ sediment activities compared to
60
all downstream Tributary A sites ($p<0.05$) with 4.5 and 8.6 times activities at the most downstream

1
2
3 Tributary A site, A4, respectively. Tributary A sites, when compared to furthest downstream site A4,
4 remained significantly higher ($p < 0.05$) at sites A1 and A2 until A3, a distance of 60 km downstream of
5 the produced water stream confluence, where there was no significant difference with site A4 activities.
6
7 DC-1 had significantly higher $^{226}\text{Ra} + ^{228}\text{Ra}$ sediment activities ($p < 0.05$) than the Reference site (6.6 times)
8 and produced water stream sites DC-3 and DC-4 (Figure 3A). DB-2.0 sediment $^{226}\text{Ra} + ^{228}\text{Ra}$ activities
9 (Figure 4A) were 26.7 times Reference site sediments and 51.8 times Reference ^{226}Ra activities,
10
11 consistent with findings from the Williston Basin pipeline fluid spill where dissolved radium activities
12 were relatively low around 0.33 Bq/L but sediments accumulated much of the radium.^{24,25} However, as
13 with dissolved Ra activities, DB-2.1 approximately 1 km downstream remained only 2.9 times Reference
14 site sediment $^{226}\text{Ra} + ^{228}\text{Ra}$ activities and 5.9 times Reference site sediment ^{226}Ra activities. According to
15 action level threshold 40 CFR 192 for the upper 15 cm of soil, sediment activities should not exceed 185
16 Bq/kg (5 pCi/g) above background – for which all NPDES facilities in this study exceeded as well as
17 produced water stream sites DB-2.1 and DC-2.
18
19

20
21 Ratios of $^{228}\text{Ra}/^{226}\text{Ra}$ in sediment samples versus distance from the discharge were plotted for DA-1
22 (Figure 2B), DC-1 (Figure 3B) and DB 2.0 (Figure 4B) with a horizontal dashed line indicating the ratio of
23 the NPDES produced water fluid (i.e., effluent). Once the ^{226}Ra and ^{228}Ra are separated from parent
24 material by chemical precipitation and deposition in the stream both radioisotopes will decay with a
25 rapid decrease in ^{228}Ra compared to ^{226}Ra , because of the difference in half-lives. The initial ratio can
26 help fingerprint sources of contamination and, in this case, indicate higher ^{226}Ra in the produced water
27 than natural background ^{228}Ra . Reference site $^{228}\text{Ra}/^{226}\text{Ra}$ in sediment ranged from 1.3-1.7, with an
28 average of 1.5 (Table 1), while sediments at sampled discharges (DA-1, DC-1, and DB 2.0) had ratios
29 below 1 with an excess of ^{226}Ra , which often indicates O&G contamination. $^{228}\text{Ra}/^{226}\text{Ra}$ ratios increase
30 with distance downstream as ^{226}Ra activities mix with natural sediments and activities return to
31 background levels (Figure S3). Interestingly, upstream River B site B1 had very low ^{226}Ra activities but
32 average sediment $^{228}\text{Ra}/^{226}\text{Ra}$ of 6.7 (Table 1) was the highest measured in the study indicating high ^{228}Ra
33 relative to ^{226}Ra (average sediment ^{228}Ra activities were 4.7 times Reference site ^{228}Ra activities). Site B1
34 was located downstream of a major agricultural irrigation diversion and dam on River B. Studies have
35 reported higher ^{228}Ra flux from fine-grained, non-carbonate sediments with higher parent material ^{232}Th
36 and increased rates of porewater exchange through sediment turbidation and agricultural associated
37 radium in phosphate fertilizers.^{66,67}
38
39
40
41
42
43
44
45
46
47
48
49
50
51
52
53
54
55
56
57
58
59
60

1
2
3 Long flow distances in combination with wetland complexes and stock ponds kilometers downstream
4 from NPDES facilities were not sampled during this study, but may provide buffering as produced water
5 streams reach equilibrium temperatures and concentrations prior to mixing with the larger rivers.
6
7 Despite this benefit, accumulation of the evaporated salt, mineral precipitates, hydrocarbon
8 compounds, and radium in sediments may potentially occur and impact endangered regional wildlife
9 and migratory birds using the O&G produced-water created wetlands as stopover habitat as evidenced
10 in bioaccumulation of these components in bird bones studied in Wyoming.⁶⁸ The radioactive scaling
11 and precipitates accumulating in sediments may pose long-term secondary sources of contamination to
12 freshwater long after produced water discharges have ceased and potentially impact freshwater biota
13 such as freshwater mussels that were observed to bioaccumulate metals associated with O&G produced
14 water in Pennsylvania streams.⁶⁹

21 22 *Changes in Radium Activity with Depth of Sediment*

23
24 Sediment radium activities were analyzed with depth to both help quantify the extent of radium
25 accumulation in the streambed and assess possible implications for groundwater. The cores collected at
26 sites DA-2 and DB-2.1 show little change in ²²⁶Ra activity with depth compared to surface grab samples
27 which ranged from 44-62 Bq/kg (Figure 5A). DC-1 ²²⁶Ra activities peaked at 925 Bq/kg (~19 times
28 background) at a depth of 18 cm while DC-1 100m and DA-3 peak at 10 and 12 cm respectively. The
29 shapes of the activity profiles remain the same when considering ²²⁶Ra + ²²⁸Ra except that they shift
30 towards higher activities (Figure S4. Core radium activities did not decrease to background grab
31 sediment activities even at depth. When observing ²²⁸Ra/²²⁶Ra ratios with depth all core sites have ratios
32 less than the Reference site grab sediment ratio of ~1.5 though DA-2 rapidly approaches background
33 ratios at a depth of around 8 cm (Figure 5B). The low ²²⁸Ra/²²⁶Ra ratios compared to background reflect
34 the low Th/U ratio in the O&G formation and the decay of the short-lived ²²⁸Ra can be observed at the
35 depth of the ²²⁶Ra peak in the DA-3, DC-1 and DC-1 100m profiles. Assuming consistent sedimentation
36 rate and a deep enough sample to remain unaffected by current radium deposition, a ²²⁸Th/²²⁸Ra age
37 dating technique was applied to the DC-1 core peak at 18 cm depth, as described by Lauer and Vengosh
38 (2016), and the sediment age was estimated to be 5 years.⁵⁵

39
40
41
42
43
44
45
46
47
48
49
50
51
52
53
54
55
56
57
58
59
60
When considering the action level for uranium and thorium mill tailings and using the Reference site
maximum measured ²²⁶Ra sediment activity of 65 Bq/kg (compared to average of 52 Bq/kg), the
regulatory limit for the upper 15 cm of soil is 250 Bq/kg and the limit below 15 cm is 620 Bq/kg. Sites

1
2
3 DA-2 and DB-2.1 meet both regulatory criteria (Figure 5A). Sites DA-3, DC-1 and DC-1 100m fail to meet
4 the regulatory limit in the upper 15 cm and DC-1 additionally fails to meet the below 15 cm regulatory
5 limit. As with radium activities rapidly decreasing with distance downstream from the discharge, DC-1
6 100m core also reflects lower activities with depth within a short distance downstream from the
7 discharge pipe. Though DB-2.1 was collected in a wetland-like holding pond around 1 km downstream of
8 the highest measured radium activities in the study at DB-2.0, the radium activities with depth were
9 below regulatory standards indicating the rapid attenuation of radium away from the point of discharge.
10
11
12
13
14
15

16 Porewater major cation concentrations for each sediment core were observed for changes with depth
17 (Table S3). Figure S5 shows the DC-1 porewater concentrations with depth and a distinct peak in
18 manganese concentrations of 120 ppb around 22 cm in depth – in coordination with ^{226}Ra peaks at the
19 same depth. Ra is known to sorb readily to manganese and iron oxides, though manganese oxide is
20 often shown to preferably sorb Ra.³¹ Iron concentrations taking method detection limits into
21 consideration, were non-detectable, though Fe(III) precipitation is likely to occur at the porewater pH
22 between 7 and 9 in conjunction with very low (non-detectable) porewater iron concentrations. Ca
23 concentrations remained high throughout the DC-1 core with a small peak around 20 cm in depth and
24 low Ba concentrations as much as 3 orders of magnitude less than Ca concentrations. The manganese
25 concentration peak at depth, consistently high calcium concentrations, and barium concentrations that
26 approach limits of detection in the porewater provide interesting insight into the potential geochemical
27 controls on Ra associations in O&G systems where low Ba concentrations could inhibit the well-studied
28 precipitation of recalcitrant barite minerals and instead allow sorption of Ra with manganese oxides, or
29 coprecipitation with calcium carbonate minerals to become the dominant Ra sequestration
30 mechanism(s).^{5,32,33}
31
32
33
34
35
36
37
38
39
40
41
42

43 *Mechanisms Controlling Radium Accumulation in Sediment*

44 Modeling progressive evaporation and chemical precipitation of solid solutions downstream of
45 discharges can generally explain the observed downstream trends (Figure S6). Conservative
46 evaporation of discharges DB-2.0 and DC-1 adequately explains the observed increases in SC and
47 concentrations of TDS, Cl, and, to a lesser extent, SO_4 and Sr downstream of the discharge, but fails to
48 explain the observed changes in pH and concentrations of Ca, Ba, and Ra (Figures S7 and S8 A, C, E),
49 whose concentrations are less than predicted by simple evaporation. However, the model that
50 combines evaporation with geochemical reactions, including equilibration with the atmosphere and
51
52
53
54
55
56
57
58
59
60

1
2
3 chemical precipitation of $(\text{Ca,Ra})\text{CO}_3$ and $(\text{Ba,Ra})\text{SO}_4$ solid-solutions, effectively simulates the observed
4 changes in pH, Ca, and Ra, including the general trends for Ba (Figures S7 and S7 B,D,F). The equilibrium
5 model over predicts the removal of Ba; observed concentrations are supersaturated with respect to
6 barite and associated solid solutions. Additional simulations indicated that (1) increasing barite
7 solubility by 0.5 log units or (2) adsorption of Ba and Sr by 100 mg/L each of HFO and HMO had a
8 negligible effect on the potential for Ba or Ra attenuation or associated mineral precipitation. Although
9 large additions of HMO sorbent have been shown to effectively bind Ba and Sr, which decreases the
10 corresponding saturation states for minerals such as barite and celestite, our porewater data indicate
11 very low concentrations of Fe and Mn in the stream sediments (Table S3) and, thus, do not support
12 modifications to the model that enhance adsorption by HFO or HMO.³¹

13
14
15
16
17
18
19
20 Based on modeling results, radium attenuation resulted from its co-precipitation with both aragonite
21 and barite, as $(\text{Ca,Ra})\text{CO}_3$ and $(\text{Ba,Ra})\text{SO}_4$ solid solutions, respectively. In both modeled cases, the
22 estimated mole fraction of RaCO_3 in $(\text{Ca,Ra})\text{CO}_3$ was 4 to 6 orders of magnitude less than the
23 corresponding mole fraction of RaSO_4 in $(\text{Ba,Ra})\text{SO}_4$ (Figure S9 C,D). Nevertheless, the estimated mass
24 of $(\text{Ca,Ra})\text{CO}_3$ precipitated was approximately 3 orders of magnitude greater than that of $(\text{Ba,Ra})\text{SO}_4$
25 (Figure S9 A,B). Thus, the indicated removal of radium with aragonite and the relative abundance of the
26 carbonate phase in the precipitated solids would be substantial, as indicated by XRD of sediments
27 (Figure 6). The evaporation models overpredict the removal of barium compared to measured
28 concentrations, thus, the computed mass of $(\text{Ba,Ra})\text{SO}_4$ precipitated and the corresponding fraction of
29 radium removed with the sulfate solid-solution phase were overpredicted. Consequently, removal of
30 radium with the carbonate phase may be underpredicted, as the aqueous radium would be available to
31 precipitate as $(\text{Ca,Ra})\text{CO}_3$.

32
33
34
35
36
37
38
39
40
41 We compared the predicted model results to observations of mineralogy in sediments using XRD.
42
43 Though barite, strontianite, and celestite were indicated to be supersaturated (Figure S6), XRD results
44 (Figure 6) detected only small percentages by weight of less than 5% each of strontianite and barite in
45 the fine sand and silt+clay fractions respectively in sample DB-2.0. Ewaldite $(\text{Ba,Ca}(\text{CO}_3)_2)$ and
46 strontianite represented <5% and 11% each of the fine sand and silt+clay fractions of sample DB-2.1.
47
48 However, when the grain-sized results (Table S4) combined to form the total sample mineralogy, the
49 barite, ewaldite, and strontianite comprised no more than 1% of the total sample by weight. Dolomite
50 was present in many of the samples with substantial compositions in samples DB-2.0, DB-2.1 and DB-2.2
51 with respective compositions of 7, 9 and <5%. Background samples were more heterogeneous in
52
53
54
55
56
57
58
59
60

1
2
3 mineral and clay composition than were DB-2.0 and DC-1 discharge sediments and subsequent
4 produced water stream sites. Discharge site DC-1 was almost completely calcium carbonate dominated
5 (>99%), including both calcite and aragonite, with minor quartz (<1%). Calcium carbonate content
6 decreased with distance downstream from the discharge to DC-3 to where none was detected. DB-2.0
7 also had a high composition of calcium carbonate (63%) at the discharge though more diversity in
8 carbonate, sulfate, and silicate minerals than DC-1. Background sediments at the Reference site
9 contained much more clay and silicate minerals than carbonates and sulfates. Linear regressions on the
10 bulk sediment sample for total $^{226}\text{Ra} + ^{228}\text{Ra}$ versus percent by weight calcium carbonate were weakly
11 significant ($p=0.09$) for all samples; however, for the DC-1 produced water stream alone ($n=3$ and thus
12 not statistically relevant) the R^2 associated with increasing radium activity and increasing calcium
13 carbonate composition by weight was 0.97. $^{226}\text{Ra} + ^{228}\text{Ra}$ vs percent by weight clay mineral compositions
14 were not significant ($p \gg 0.05$).

23
24 Sediment leaching was completed to better understand radium association with operationally defined
25 solid phases. Only the Reference site sample lost more than 8% of the total ^{226}Ra activity after the first
26 leach step targeting soluble salts (~20% loss) (Figure 7). Leach step two targeting exchangeable ions on
27 clay minerals produced varied results, with DC-1, DC-2 and DB-2.0 samples still maintaining over 80% of
28 the total ^{226}Ra activity while River C sites and other produced water sites downstream lost larger
29 percentages of ^{226}Ra activity. Muscovite, detected by XRD at high percentages in some samples can sorb
30 large amounts of Ra while quartz and other silicate mineral compositions of sediments absorb less,
31 confirming that background samples with high quartz compositions preferentially sorb Ra to clay
32 minerals during accumulation.^{70,71} Additionally, Ra adsorbed to carbonate surfaces could potentially
33 desorb during this step.⁵⁰ Sample DC-1 lost approximately 75% of the total ^{226}Ra activity and 97% of total
34 sample mass after the third leaching step with acetic acid targeting carbonate minerals. This was
35 expected with DC-1 composed approximately 100% of calcium carbonate minerals. DC-2 lost about 70%,
36 DB-2.0 63% and DB-2.1 approximately 42% of total ^{226}Ra activity after the third leach. It is important to
37 note that application of acetic acid in step 3 could have promoted desorption of Ra from iron and
38 manganese oxides, which would otherwise dissolve in HCl during step 4. Leachate chemistry results
39 (Table S5) demonstrate that Mn and Fe were partly mobilized during the acetic acid step 3. However,
40 the calcium concentrations in step 3 leachates were three orders of magnitude larger than iron and
41 manganese concentrations, and proportionally greater amounts of manganese and iron than calcium
42 were released during step 4. Combined, the leaching results indicate that the majority of radium is likely
43
44
45
46
47
48
49
50
51
52
53
54
55
56
57
58
59
60

1
2
3 coprecipitated with calcium carbonates at the NPDES discharges, with smaller fractions associated with
4 iron and manganese oxides, all of which could release radium to waters with low pH. To confirm
5 complete carbonate dissolution, leachates from samples DC-1 and DB-2.0 accounted for 99% and 96% of
6 the sample calcium, respectively. Sample DC-1 only lost 1% ²²⁶Ra after leach step four though DB-2.0 lost
7 approximately 8% and downstream sites lost between 10-15% to the acid soluble fraction including Fe
8 and Mn oxides. SEM and EDS elemental mapping for DC-1 and DB-2.0 leach four residues (Figure S11
9 and S12) show no visible association between Sr, Ca, or S with little to no Ba present. Sr present in DB-
10 2.0 residues were likely associated as exchangeable ions on clay particles (Si and Al).

11 Although water sampling captured a range of base-flow conditions between 2013-2016, additional
12 sampling may be needed to document radium transport during high-flow conditions and corresponding
13 annual discharge quantities. Additionally, although sediment samples were collected to shallow depths
14 along downstream transects twice in 2016, repeated sampling at other times and greater depths may be
15 needed to provide high resolution on a temporal scale. The sequential extraction, mineralogical, and
16 geochemical modeling results consistently indicated significant associations between radium and
17 carbonate solids. However, additional work may be appropriate to determine the precise compositions
18 and mineralogy of the relevant phases, including low concentrations of sulfate minerals, if radium is
19 primarily contained within the solid matrix or adsorbed on surfaces, and if identified carbonate (and
20 sulfate) solid solutions remain stable or tend to recrystallize into pure component phases over time or as
21 geochemical conditions vary.

22 Future studies may be considered to evaluate possible management scenarios to reduce radium
23 transport from the produced water discharge sites. For example, increasing aeration in O&G holding
24 tanks and ponds already in existence could increase dissolved oxygen concentrations, encourage radium
25 adsorption with precipitated iron and manganese oxides, or its coprecipitation into carbonate and
26 sulfate minerals. Aeration of the discharges would tend to increase oxygen concentrations and increase
27 pH, which favors the kinetics of iron and manganese oxidation as well as carbonate precipitation.

28 Additionally, the construction of low energy areas of sediment deposition such as in wetland complexes
29 where radium could be sorbed to iron and manganese oxides, buried as carbonate and/or barite solid
30 solution particles, and bioaccumulated in vegetation may be evaluated with consideration of possible
31 impacts to wildlife and livestock. Lastly, various sources of NORM other than O&G extraction activities
32 could be inventoried and evaluated to gain a greater understanding of possible contributions on a
33 regional scale.

34 **Conclusion**

35
36
37
38
39
40
41
42
43
44
45
46
47
48
49
50
51
52
53
54

1
2
3 The NPDES facilities in this study met dissolved ^{226}Ra effluent regulatory criteria of 2.22 Bq/L (60 pCi/L) –
4 both permit-reported and measured. However, lower activities of $^{226}\text{Ra} + ^{228}\text{Ra}$ in effluent can still lead
5 to accumulation of high activities of $^{226}\text{Ra} + ^{228}\text{Ra}$ in sediments near outfalls, as noted in this and other
6 produced water discharge studies.^{5,13,23–25} Sediments at discharges in this study had activities for ^{226}Ra
7 nearing 50 times those for background and reference site conditions, whereas values only 5 times
8 background activities exceed action level thresholds. It is important to stress that the sediments studied
9 were not from spill sites but from constant sources of low-level contamination releasing billions of Bq of
10 radium activity to the environment every year.
11
12

13
14
15
16
17 While the elevated sediment and dissolved radium activities in the water decrease rapidly downstream,
18 the resulting toxicity and health impacts associated with discharges utilized for livestock watering and
19 wildlife propagation remains largely unstudied. Sediment radium accumulation may lead to a long-term
20 ecological footprint when aquatic biota or migratory birds using O&G wetland complexes, permitted as
21 beneficial reuse of produced water, beyond the scope of this study, as flyover habitat are exposed to
22 chronic high sediment radium activities.¹ Agricultural repurposing of produced water may not be
23 justifiable for wildlife propagation where radium accumulates within sensitive organisms (e.g.,
24 freshwater mussels) via external contact or ingestion, though mortality and growth inhibition effects
25 remain unknown.⁶⁹
26
27
28
29
30
31
32

33 Radium co-precipitation with carbonate minerals deduced in this field study of western U.S. produced
34 water discharges would create a reservoir of secondary source contamination. As equilibrium conditions
35 shift with episodic dilution and acidification, the carbonate-associated radium would tend to dissolve.
36 Acidic rainwater and snowmelt runoff thus may release previously sequestered radium back to the
37 water column where bioavailable for both animals and humans.^{51,57}
38
39
40
41
42

43 Due to the rapid attenuation of Ra towards background activities within short distances downstream of
44 NPDES facilities, but with apparent accumulation in stream sediments that remain mobile, potential
45 solutions to continue beneficial use practices according to 40 CFR § 435 Subpart E from a Ra standpoint
46 could include construction of low-maintenance wetlands/infiltration ponds below points of discharge.
47 This would allow for establishment of collection areas for radium accumulation under chemical and
48 equilibrium conditions (i.e. temperature stabilization and increased oxygen concentrations) and reduce
49 transport of radium in the receiving streams. Infrequently, sediments with associated radium could be
50 removed and disposed as appropriate.
51
52
53
54
55
56
57
58
59
60

Conflicts of Interest

There are no conflicts of interest to declare.

Acknowledgements

We gratefully acknowledge Johnna Puhr, Yadiel Varela Soler and Sydney Page for assistance with grab and core sediment preparation, Travis Tasker for analyzing samples with the ICP-AES, and O&G collaborators without whom this project could not have taken place.

References

- 1 K. Guerra, K. Dahm and S. Dundorf, *Oil and gas produced water management and beneficial use in the Western United States*, Science and Technology Program Report No. 157, US Department of Interior, Bureau of Reclamation, Denver, USA 2011.
- 2 F. C. Dolan, T. Y. Cath and T. S. Hogue, Assessing the feasibility of using produced water for irrigation in Colorado, *Sci. Total Environ.*, 2018, **640–641**, 619–628.
- 3 T. A. Blewett, P. L. M. Delompré, C. N. Glover and G. G. Goss, Physical immobility as a sensitive indicator of hydraulic fracturing fluid toxicity towards *Daphnia magna*, *Sci. Total Environ.*, 2018, **635**, 639–643.
- 4 T. A. Blewett, A. M. Weinrauch, P. L. M. Delompré and G. G. Goss, The effect of hydraulic flowback and produced water on gill morphology, oxidative stress and antioxidant response in rainbow trout (*Oncorhynchus mykiss*), *Sci. Rep.*, 2017, **7**, 46582.
- 5 N. R. Warner, C. A. Christie, R. B. Jackson and A. Vengosh, Impacts of shale gas wastewater disposal on water quality in Western Pennsylvania, *Environ. Sci. Technol.*, 2013, **47**, 11849–11857.
- 6 C. D. Kassotis, L. R. Iwanowicz, D. M. Akob, I. M. Cozzarelli, A. C. Mumford, W. H. Orem and S. C. Nagel, Endocrine disrupting activities of surface water associated with a West Virginia oil and gas industry wastewater disposal site, *Sci. Total Environ.*, 2016, **557–558**, 901–910.
- 7 J. S. Harkness, G. S. Dwyer, N. R. Warner, K. M. Parker, W. A. Mitch and A. Vengosh, Iodide, Bromide, and Ammonium in Hydraulic Fracturing and Oil and Gas Wastewaters: Environmental Implications, *Environ. Sci. Technol.*, 2015, **49**, 1955–1963.
- 8 K. M. Parker, T. Zeng, J. Harkness, A. Vengosh and W. A. Mitch, Enhanced Formation of Disinfection Byproducts in Shale Gas Wastewater-Impacted Drinking Water Supplies, *Environ. Sci. Technol.*, 2014, **48**, 11161–11169.
- 9 K. J. Ferrar, D. R. Michanowicz, C. L. Christen, N. Mulcahy, S. L. Malone and R. K. Sharma, Assessment of effluent contaminants from three facilities discharging marcellus shale wastewater to surface waters in Pennsylvania, *Environ. Sci. Technol.*, , DOI:10.1021/es301411q.
- 10 G. J. Getzinger, M. P. O'Connor, K. Hoelzer, B. D. Drollette, O. Karatum, M. A. Deshusses, P. L. Ferguson, M. Elsner and D. L. Plata, Natural Gas Residual Fluids: Sources, Endpoints, and Organic Chemical Composition after Centralized Waste Treatment in Pennsylvania, *Environ. Sci. Technol.*,

- 2015, **49**, 8347–8355.
- 11 M. L. Hladik, M. J. Focazio and M. Engle, Discharges of produced waters from oil and gas extraction via wastewater treatment plants are sources of disinfection by-products to receiving streams, *Sci. Total Environ.*, 2014, **466**, 1085–1093.
- 12 J. M. Wilson and J. M. Vanbriesen, Oil and Gas Produced Water Management and Surface Pennsylvania, *Environ. Pract.*, 2012, **14**, 288–301.
- 13 N. E. Lauer, N. R. Warner and A. Vengosh, Sources of Radium Accumulation in Stream Sediments near Disposal Sites in Pennsylvania: Implications for Disposal of Conventional Oil and Gas Wastewater, *Environ. Sci. Technol.*, 2018, **52**, 955–962.
- 14 A. Vengosh, *Salinization and Saline Environments*, Elsevier Ltd., 2nd edn., 2013, vol. 11.
- 15 E. L. Rowan, M. a. Engle, C. S. Kirby and T. F. Kraemer, Radium Content of Oil- and Gas-Field Produced Waters in the Northern Appalachian Basin (USA): Summary and Discussion of Data, *USGS Sci. Investig. Rep.*, 2011, 38 pp.
- 16 K. Oetjen, J. Blotevogel, T. Borch, J. F. Ranville and C. P. Higgins, Simulation of a hydraulic fracturing wastewater surface spill on agricultural soil, *Sci. Total Environ.*, 2018, **645**, 229–234.
- 17 United Nations, *Sources and Effects of Ionizing Radiation United Nations Scientific Committee on the Effects of Atomic Radiation*, New York, 2011, vol. II.
- 18 F. Carvalho, D. Chambers, S. Fesenko, W. S. Moore, D. Porcelli, H. Vandenhoven and T. Yankovich, *Environmental Pathways and Corresponding Models*, Vienna, 2014.
- 19 National Research Council, *Health Effects of Exposure to Radon*, National Academies Press, 1999.
- 20 US Nuclear Regulatory Commission, *Appendix B to Part 20 Annual Limits on Intake (ALIs) and Derived Air Concentrations (DACs) of Radionuclides for Occupational Exposure; Effluent Concentrations; Concentrations for Release to Sewerage*, 2017.
- 21 US Environmental Protection Agency, *National Interim Primary Drinking Water Regulations*, Washington, DC, 1976.
- 22 J. Rosenblum, A. W. Nelson, B. Ruyle, M. K. Schultz, J. N. Ryan and K. G. Linden, Temporal characterization of flowback and produced water quality from a hydraulically fractured oil and gas well, *Sci. Total Environ.*, 2017, **596–597**, 369–377.
- 23 W. D. Burgos, L. Castillo-Meza, T. L. Tasker, T. J. Geeza, P. J. Drohan, X. Liu, J. D. Landis, J. Blotevogel, M. McLaughlin, T. Borch and N. R. Warner, Watershed-Scale Impacts from Surface Water Disposal of Oil and Gas Wastewater in Western Pennsylvania, *Environ. Sci. Technol.*, 2017, **51**, 8851–8860.
- 24 I. M. Cozzarelli, K. J. Skalak, D. B. Kent, M. A. Engle, A. Benthem, A. C. Mumford, K. Haase, A. Farag, D. Harper, S. C. Nagel, L. R. Iwanowicz, W. H. Orem, D. M. Akob, J. B. Jaeschke, J. Galloway, M. Kohler, D. L. Stoliker and G. D. Jolly, Environmental signatures and effects of an oil and gas wastewater spill in the Williston Basin, North Dakota, *Sci. Total Environ.*, 2016, **579**, 1781–1793.
- 25 N. E. Lauer, J. S. Harkness and A. Vengosh, Brine Spills Associated with Unconventional Oil

- 1
2
3 Development in North Dakota, *Environ. Sci. Technol.*, 2016, acs.est.5b06349.
4
5 26 International Atomic Energy Agency, *The Environmental Behaviour of Radium : Revised Edition*,
6 Vienna, 2014.
7
8 27 C. A. Menzie, B. Southworth, G. Stephenson and N. Feisthauer, The importance of understanding
9 the chemical form of a metal in the environment: The case of barium sulfate (barite), *Hum. Ecol.*
10 *Risk Assess.*, 2008, **14**, 974–991.
11
12 28 B. Ouyang, D. M. Akob, D. Dunlap and D. Renock, Microbially mediated barite dissolution in
13 anoxic brines, *Appl. Geochemistry*, 2017, **76**, 51–59.
14
15 29 D. Renock, J. D. Landis and M. Sharma, Reductive weathering of black shale and release of barium
16 during hydraulic fracturing, *Appl. Geochemistry*, 2016, **65**, 73–86.
17
18 30 E. R. Elizabeth J. P. Phillips, Sulfate-Reducing Bacteria Release Barium and Radium from Naturally
19 Occurring Radioactive Material in Oil-Field Barite, *Geomicrobiol. J.*, 2001, **18**, 167–182.
20
21 31 K. Van Sice, C. A. Cravotta, B. McDevitt, T. L. Tasker, J. Landis, J. Pühr and N. R. Warner, Radium
22 fate following oil and gas wastewater disposal to western Pennsylvania surface waters, *Appl.*
23 *Geochemistry*, In Press.
24
25 32 T. Zhang, K. Gregory, R. W. Hammack and R. D. Vidic, Co-precipitation of radium with barium and
26 strontium sulfate and its impact on the fate of radium during treatment of produced water from
27 unconventional gas extraction, *Environ. Sci. Technol.*, 2014, **48**, 4596–4603.
28
29 33 T. Zhang, R. W. Hammack and R. D. Vidic, Fate of Radium in Marcellus Shale Flowback Water
30 Impoundments and Assessment of Associated Health Risks, *Environ. Sci. Technol.*, 2015, **49**,
31 9347–9354.
32
33 34 M. Sajih, N. D. Bryan, F. R. Livens, D. J. Vaughan, M. Descostes, V. Phommavanh, J. Nos and K.
35 Morris, Adsorption of radium and barium on goethite and ferrihydrite: A kinetic and surface
36 complexation modelling study, *Geochim. Cosmochim. Acta*, 2014, **146**, 150–163.
37
38 35 A. Vengosh, R. B. Jackson, N. Warner, T. H. Darrah and A. Kondash, A critical review of the risks to
39 water resources from unconventional shale gas development and hydraulic fracturing in the
40 United States, *Environ. Sci. Technol.*, 2014, **48**, 8334–8348.
41
42 36 A. J. Kondash, N. R. Warner, O. Lahav and A. Vengosh, Radium and barium removal through
43 blending hydraulic fracturing fluids with acid mine drainage, *Environ. Sci. Technol.*, 2014, **48**,
44 1334–1342.
45
46 37 F. Grandia, J. Merino and J. Bruno, Assessment of the radium-barium co-precipitation and its
47 potential influence on the solubility of Ra in the near-field, 2008, **TR-08-07**, 52.
48
49 38 C. He, M. Li, W. Liu, E. Barbot and R. D. Vidic, Kinetics and Equilibrium of Barium and Strontium
50 Sulfate Formation in Marcellus Shale Flowback Water, *J. Environ. Eng.*, 2014, ,
51 DOI:10.1061/(ASCE)EE.1943-7870.0000807.
52
53 39 D. Langmuir and D. Melchior, The geochemistry of Ca, Sr, Ba and Ra sulfates in some deep brines
54 from the Palo Duro Basin, Texas, *Geochim. Cosmochim. Acta*, 1985, **49**, 2423–2432.
55
56
57
58
59
60

- 1
2
3 40 F. Brandt, E. Curti, M. Klinkenberg, K. Rozov and D. Bosbach, Replacement of barite by a
4 (Ba,Ra)SO₄ solid solution at close-to-equilibrium conditions: A combined experimental and
5 theoretical study, *Geochim. Cosmochim. Acta*, 2015, **155**, 1–15.
6
7 41 V. L. Vinograd, F. Brandt, K. Rozov, M. Klinkenberg, K. Refson, B. Winkler and D. Bosbach, Solid-
8 aqueous equilibrium in the BaSO₄-RaSO₄-H₂O system: First-principles calculations and a
9 thermodynamic assessment, *Geochim. Cosmochim. Acta*, 2013, **122**, 398–417.
10
11 42 V. L. Vinograd, D. A. Kulik, F. Brandt, M. Klinkenberg, J. Weber, B. Winkler and D. Bosbach,
12 Thermodynamics of the solid solution - Aqueous solution system (Ba,Sr,Ra)SO₄ + H₂O: I. The
13 effect of strontium content on radium uptake by barite, *Appl. Geochemistry*, 2018, **89**, 59–74.
14
15 43 V. L. Vinograd, D. A. Kulik, F. Brandt, M. Klinkenberg, J. Weber, B. Winkler and D. Bosbach,
16 Thermodynamics of the solid solution - Aqueous solution system (Ba,Sr,Ra)SO₄ + H₂O: II. Radium
17 retention in barite-type minerals at elevated temperatures, *Appl. Geochemistry*, 2018, **93**, 190–
18 208.
19
20 44 A. J. Tesoriero and J. F. Pankow, Solid solution partitioning of Sr²⁺, Ba²⁺, and Cd²⁺ to calcite,
21 *Geochim. Cosmochim. Acta*, 1996, **60**, 1053–1063.
22
23 45 E. Curti, Coprecipitation of radionuclides with calcite: Estimation of partition coefficients based
24 on a review of laboratory investigations and geochemical data, *Appl. Geochemistry*, 1999, **14**,
25 433–445.
26
27 46 D. S. Vinson, J. R. Lundy, G. S. Dwyer and A. Vengosh, Implications of carbonate-like geochemical
28 signatures in a sandstone aquifer: Radium and strontium isotopes in the Cambrian Jordan aquifer
29 (Minnesota, USA), *Chem. Geol.*, 2012, **334**, 280–294.
30
31 47 W. Back and B. B. Hanshaw, Comparison of chemical hydrogeology of the carbonate peninsulas
32 of Florida and Yucatan, *J. Hydrol.*, 1970, **10**, 330–368.
33
34 48 P. Glynn, Solid-Solution Solubilities and Thermodynamics: Sulfates, Carbonates and Halides, *Rev.*
35 *Mineral. Geochemistry*, 2000, **40**, 481–511.
36
37 49 B. B. Hanshaw and W. Back, Major geochemical processes in the evolution of carbonate-aquifer
38 systems, *Dev. Water Sci.*, 1979, **12**, 287–312.
39
40 50 M. J. Jones, L. J. Butchins, J. M. Charnock, R. A. D. Patrick, J. S. Small, D. J. Vaughan, P. L. Wincott
41 and F. R. Livens, Reactions of radium and barium with the surfaces of carbonate minerals, *Appl.*
42 *Geochemistry*, 2011, **26**, 1231–1238.
43
44 51 P. M. Dove and F. M. Platt, Compatible real-time rates of mineral dissolution by Atomic Force
45 Microscopy (AFM), *Chem. Geol.*, 1996, **127**, 331–338.
46
47 52 C. Clark and J. Veil, U.S. Produced water volumes and management practices, *Groundw. Prot.*
48 *Counc.*, 2015, 119.
49
50 53 US Environmental Protection Agency, *Rapid Radiochemical Methods for Selected Radionuclides in*
51 *Water for Environmental Restoration Following Homeland Security Events*, Montgomery, 2010.
52
53 54 US Environmental Protection Agency, *Radiochemistry Procedures Manual*, 1984.
54
55
56
57
58
59
60

- 1
2
3 55 N. Lauer and A. Vengosh, Age Dating Oil and Gas Wastewater Spills Using Radium Isotopes and
4 Their Decay Products in Impacted Soil and Sediment, *Environ. Sci. Technol. Lett.*, 2016, **3**,
5 205–209.
6
- 7 56 B. W. Stewart, E. C. Chapman, R. C. Capo, J. D. Johnson, J. R. Graney, C. S. Kirby and K. T.
8 Schroeder, Origin of brines, salts and carbonate from shales of the Marcellus Formation:
9 Evidence from geochemical and Sr isotope study of sequentially extracted fluids, *Appl.*
10 *Geochemistry*, 2015, **60**, 78–88.
11
- 12 57 T. T. Phan, R. C. Capo, B. W. Stewart, J. R. Graney, J. D. Johnson, S. Sharma and J. Toro, Trace
13 metal distribution and mobility in drill cuttings and produced waters from Marcellus Shale gas
14 extraction: Uranium, arsenic, barium, *Appl. Geochemistry*, 2015, **60**, 89–103.
15
- 16 58 D. L. Parkhurst and C. A. J. Appelo, Description of Input and Examples for PHREEQC Version 3 — A
17 Computer Program for Speciation , Batch-Reaction , One-Dimensional Transport , and Inverse
18 Geochemical Calculations. U.S. Geological Survey Techniques and Methods, book 6, chapter A43,
19 497 p., *U.S. Geol. Surv. Tech. Methods, B. 6, chapter A43*, 2013, 6–43A.
20
- 21 59 J. W. Ball and D. K. Nordstrom, User's Manual for Wateq4F, With Revised Thermodynamic Data
22 Base and Test Cases for Calculating Speciation of Major, Trace, and Redox Elements in Natural
23 Waters, *U.S. Geol. Surv. Open-File Rep. 91-183*, 1991.
24
- 25 60 E. Giffaut, M. Grivé, P. Blanc, P. Vieillard, E. Colàs, H. Gailhanou, S. Gaboreau, N. Marty, B. Madé
26 and L. Duro, Andra thermodynamic database for performance assessment: ThermoChimie, *Appl.*
27 *Geochemistry*, 2014, **49**, 225–236.
28
- 29 61 D. Langmuir and A. C. Riese, The Thermodynamic Properties of Radium, *Geochim. Cosmochim.*
30 *Acta*, 1985, **49**, 1593–1601.
31
- 32 62 R. B. McCleskey, D. K. Nordstrom, J. N. Ryan and J. W. Ball, A new method of calculating electrical
33 conductivity with applications to natural waters, *Geochim. Cosmochim. Acta*, 2012, **77**, 369–382.
34
- 35 63 Y. O. Rosenberg, Z. Sade and J. Ganor, The precipitation of gypsum, celestine, and barite and
36 coprecipitation of radium during seawater evaporation, *Geochim. Cosmochim. Acta*, 2018, **233**,
37 50–65.
38
- 39 64 R. M. Rodríguez-Galán and M. Prieto, Interaction of Nonideal, Multicomponent Solid Solutions
40 With Water: A Simple Algorithm to Estimate Final Equilibrium States, *Geochemistry, Geophys.*
41 *Geosystems*, 2018, **19**, 1348–1359.
42
- 43 65 P. Dresel and A. Rose, Chemistry and origin of oil and gas well brines in western Pennsylvania,
44 *Pennsylvania Geol. Surv., 4th Ser. Open-File Rep. OFOG 10–01.0*, 2010, 48.
45
- 46 66 D. Barišić, S. Lulić and P. Miletić, Radium and uranium in phosphate fertilizers and their impact on
47 the radioactivity of waters, *Water Res.*, 1992, **26**, 607–611.
48
- 49 67 W. S. Moore, J. L. Sarmiento and R. M. Key, Submarine groundwater discharge revealed by ²²⁸Ra
50 distribution in the upper Atlantic Ocean, *Nat. Geosci.*, 2008, **1**, 309–311.
51
- 52 68 P. J. Ramirez, Oil Field Produced Water Discharges into Wetlands in Wyoming, *US Fish and*
53 *Wildlife Service Environmental. Contamination Report R6/718C/02*, 2015.
54
55
56
57
58
59
60

- 1
2
3 69 T. J. Geeza, D. P. Gillikin, B. McDevitt, K. Van Sice and N. R. Warner, Accumulation of Marcellus
4 Formation Oil and Gas Wastewater Metals in Freshwater Mussel Shells, *Environ. Sci. Technol.*,
5 2018, 52, 10883–10892.
6
7 70 P. Benes, B. Z. and P. Strejc, Interaction of Radium With Freshwater Sediments and their Mineral
8 Components: III. Muscovite and Feldspar., *J. Radioanal. Nucl. Chem.*, 1986, **98**, 91–103.
9
10 71 P. Benes, P. Strejc and Z. Lukavec, Interaction of Radium with Freshwater Sediments and their
11 Mineral Components. I. Ferric hydroxide and quartz., *J. Radioanal. Nucl. Chem.*, 1984, **82**, 275–
12 285.
13
14
15
16
17
18
19
20
21
22
23
24
25
26
27
28
29
30
31
32
33
34
35
36
37
38
39
40
41
42
43
44
45
46
47
48
49
50
51
52
53
54
55
56
57
58
59
60

1
2
3 **Figure 1. A.** Locations of water and grab sediment sampling points near NPDES permitted discharges
4 with ephemeral streams, Tributary A, River B, River C and a reference site with no known oil and gas
5 activity or NPDES discharges. Note that all tributaries drain to a drinking water supply reservoir
6 downstream. Discharges where sediment cores were taken are denoted by stars. **B and C.** Detailed maps
7 of the DC-1 and DB-2.0 discharges and produced water streams, respectively.
8
9

10
11
12 **Figure 2A.** Total radium activities ($^{228}\text{Ra} + ^{226}\text{Ra}$) (Bq/kg) in sediment samples versus distance
13 downstream of NPDES discharge DA-1 (black squares). Note additional NPDES discharges at 9-10 km:
14 DA-2 (circles), DA-3 (diamonds), and downstream site DA-4 (open squares). Activities are most elevated
15 near the NPDES discharges and then are mixed and diluted downstream of the confluence with
16 Tributary A. **2B)** $^{228}\text{Ra}/^{226}\text{Ra}$ in sediments increase downstream of discharges to reflect mixing with
17 background activities.
18

19
20 **Figure 3A.** Total radium activities ($^{228}\text{Ra} + ^{226}\text{Ra}$) (Bq/kg) in sediment samples versus distance
21 downstream of NPDES discharge DC-1. Activities are most elevated at the NPDES discharge and then are
22 mixed and diluted downstream of a confluence with River C. **3B)** $^{228}\text{Ra}/^{226}\text{Ra}$ in sediments increase
23 downstream of discharges and are lower in the sediment than the liquid discharge effluent with a ratio
24 of 0.61, indicating accumulation of radium over a period of time. Farther downstream the ratios are high
25 as the impacted sediments mix with background sediments with higher ratios.
26
27

28
29
30 **Figure 4A.** Total radium activities ($^{228}\text{Ra} + ^{226}\text{Ra}$) (Bq/kg) in sediment samples versus distance
31 downstream of NPDES discharge DB-2.0. The highest study activities were measured at DB-2.0 but
32 quickly decrease to near background within 2 km downstream. **4B)** $^{228}\text{Ra}/^{226}\text{Ra}$ in sediments increase
33 downstream of discharges and are lower in the sediment than the liquid discharge with a ratio of 0.71,
34 indicating accumulation of radium over a period of time. Farther downstream the ratios are high as the
35 impacted sediments mix with background sediments with higher ratios.
36
37

38
39 **Figure 5A.** ^{226}Ra activities (Bq/kg) versus depth in sediment cores collected near the points of NPDES
40 permitted discharges DB-2.0, DA-1, DA-2, DA-3 and DC-1 and 100 m downstream of DC-1. Three of the 5
41 cores contained sediment concentrations above the 0-15 cm standard acceptable level above
42 background, while only 1 core, DC-1 appeared to contain sediment above the acceptable activity >15 cm
43 below the sediment-water interface. The Reference site grab sediment ^{226}Ra activity ranged from 44-62
44 Bq/kg (green bar) in the upper 5 cm. **5B.** Core DA-2 appeared to have little elevated activity and ratios
45 similar to background sediments at depths greater than 15 cm. However, most cores appear to show
46 decreased $^{228}/^{226}\text{Ra}$ ratios commonly found associated with older oil and gas wastes. The Reference Site
47 grab sediment ratio (green square) ranged from 1.3-1.7 in the upper 5 cm.
48
49
50

51
52
53 **Figure 6.** XRD results for select sediment grab samples. The composited sediments contained
54 predominantly calcium carbonate (calcite and aragonite) or silica (quartz), with an array of minor
55 percentages of other minerals, including no more than 1% barite, ewaldite, and strontianite. Note that
56
57
58
59
60

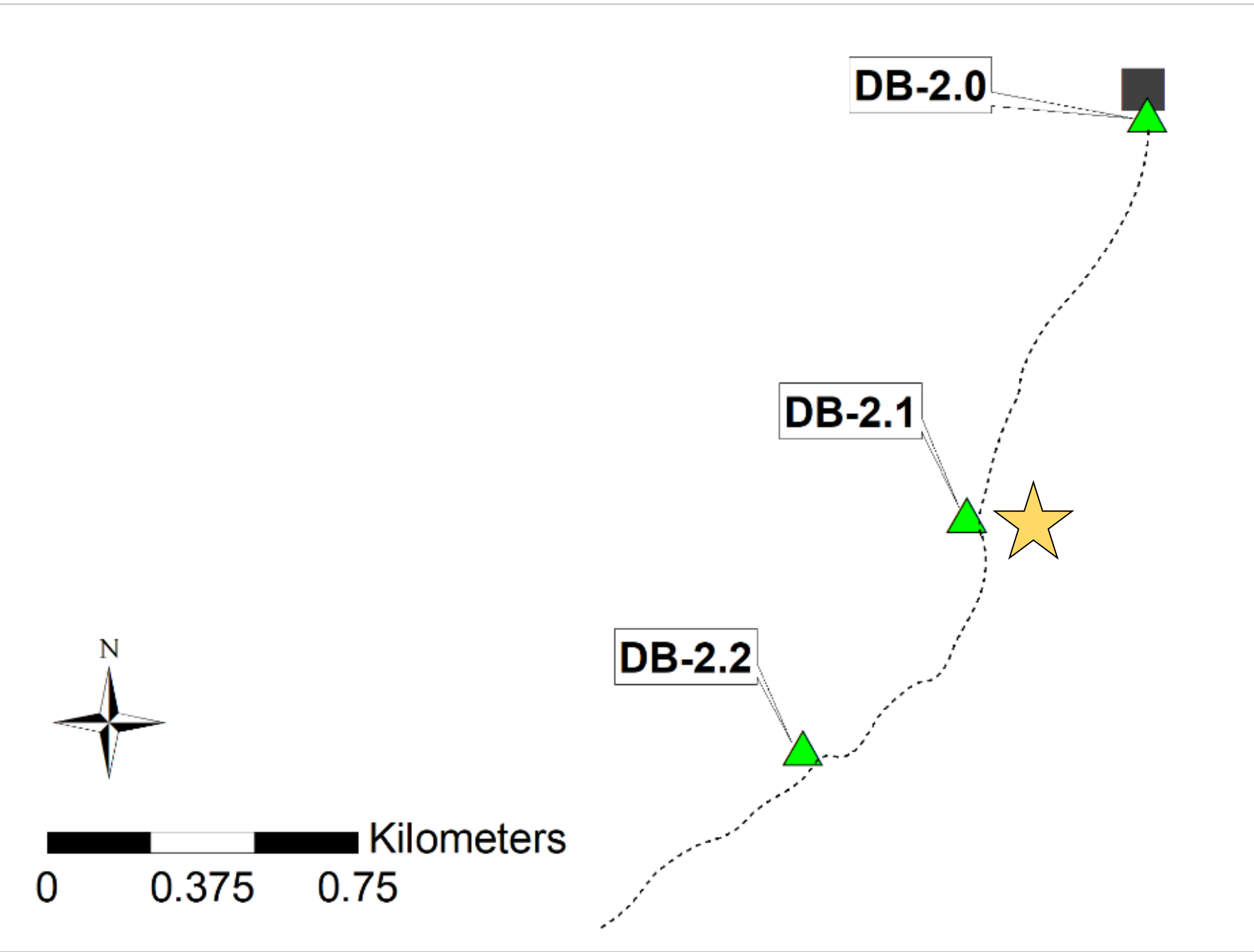
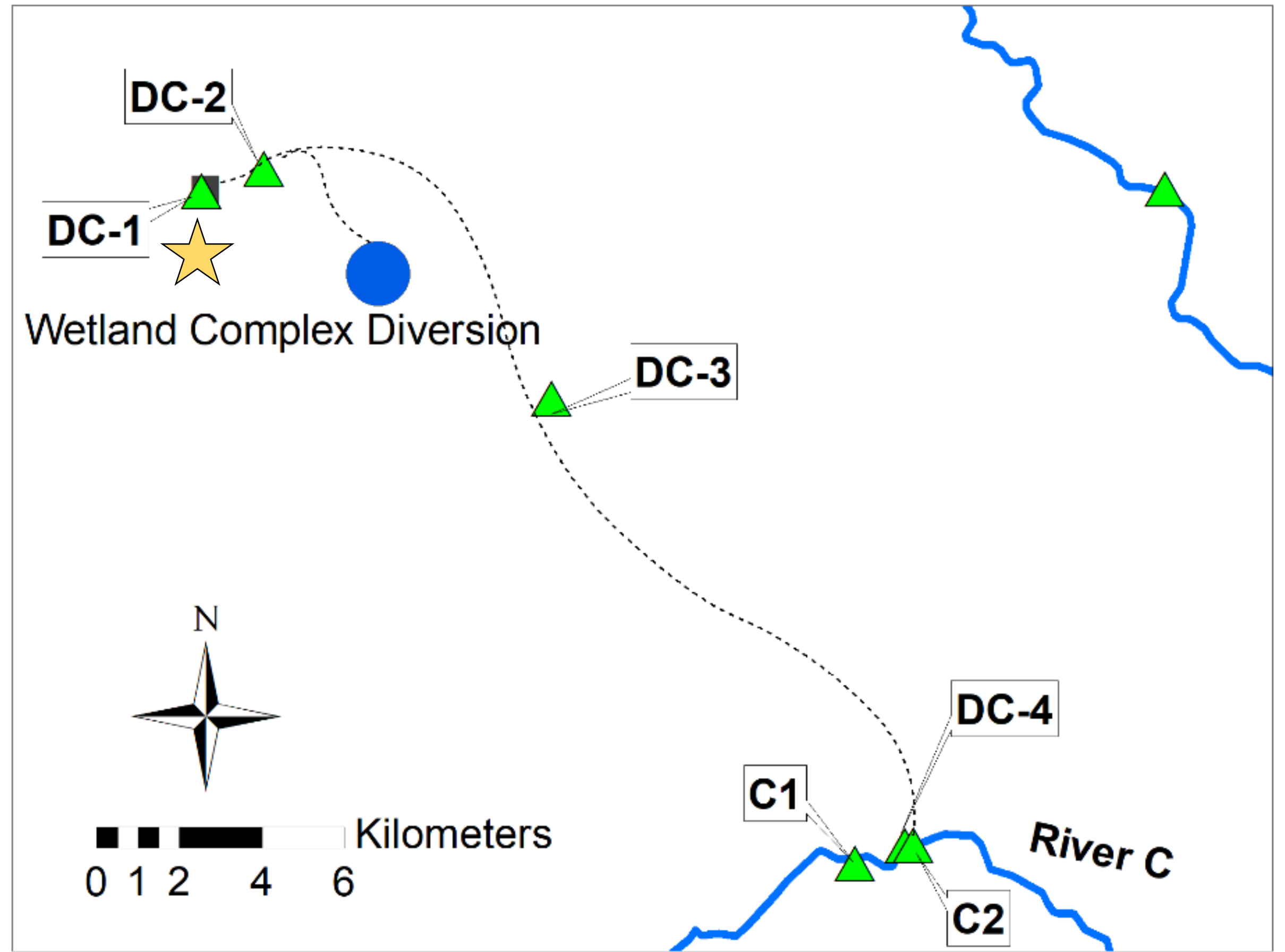
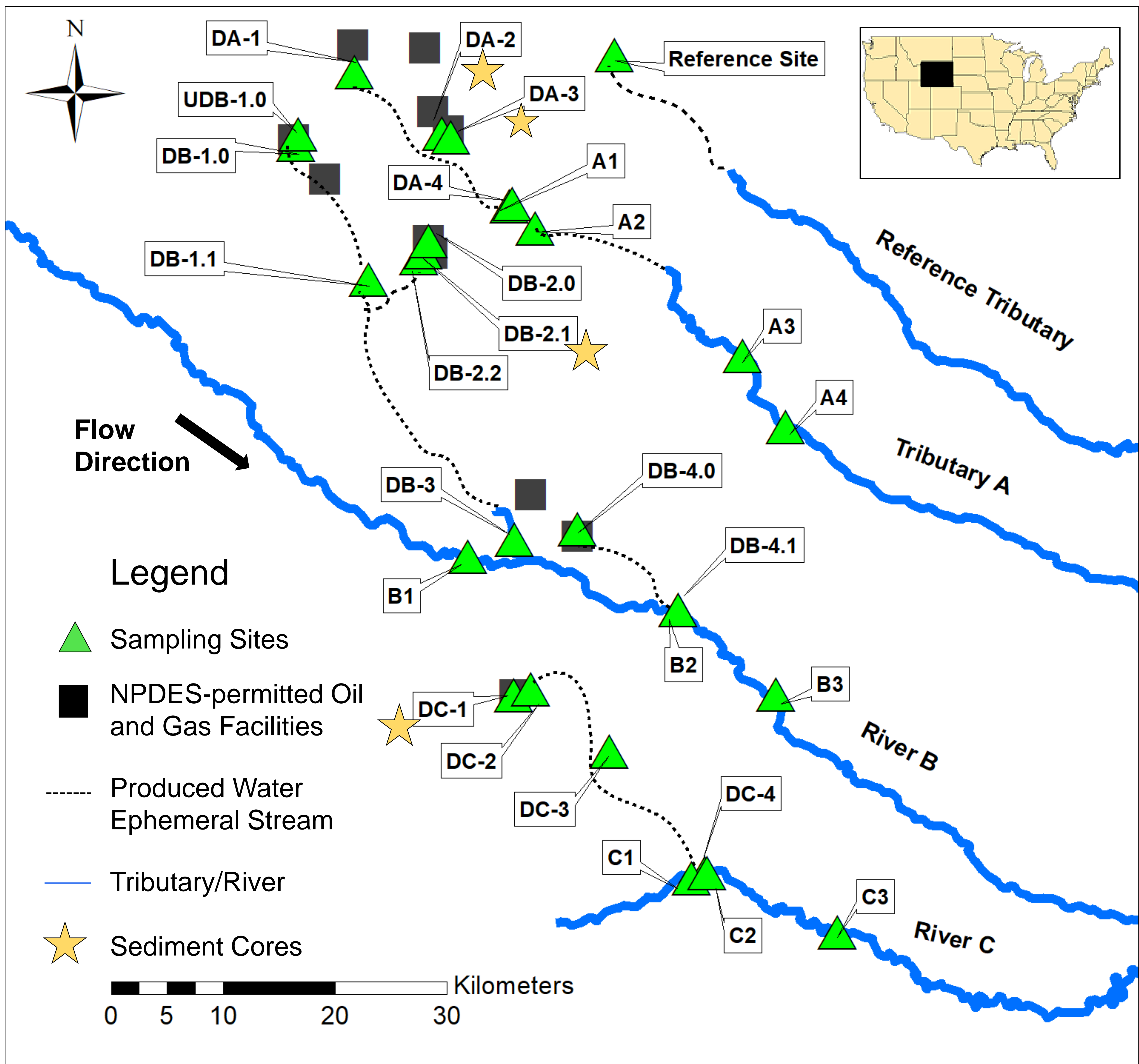
1
2
3 the sediments sampled at discharge facilities contained greater percentages of calcium carbonate and
4 lower percentages of quartz compared to background and reference sites.
5

6 **Figure 7.** Radium 226 activity in samples following liquid extraction steps normalized to values of the
7 original sediment. Note the majority of sediments collected near discharge sites contained significantly
8 less radium following extraction steps 2 (exchangeable) and 3 (carbonate). Combined, this indicates the
9 radium is present in and likely associated with easily leachable minerals such as calcium carbonate and
10 not in recalcitrant forms such as sulfates (barite and celestite).
11
12
13
14
15
16
17
18
19
20
21
22
23
24
25
26
27
28
29
30
31
32
33
34
35
36
37
38
39
40
41
42
43
44
45
46
47
48
49
50
51
52
53
54
55
56
57
58
59
60

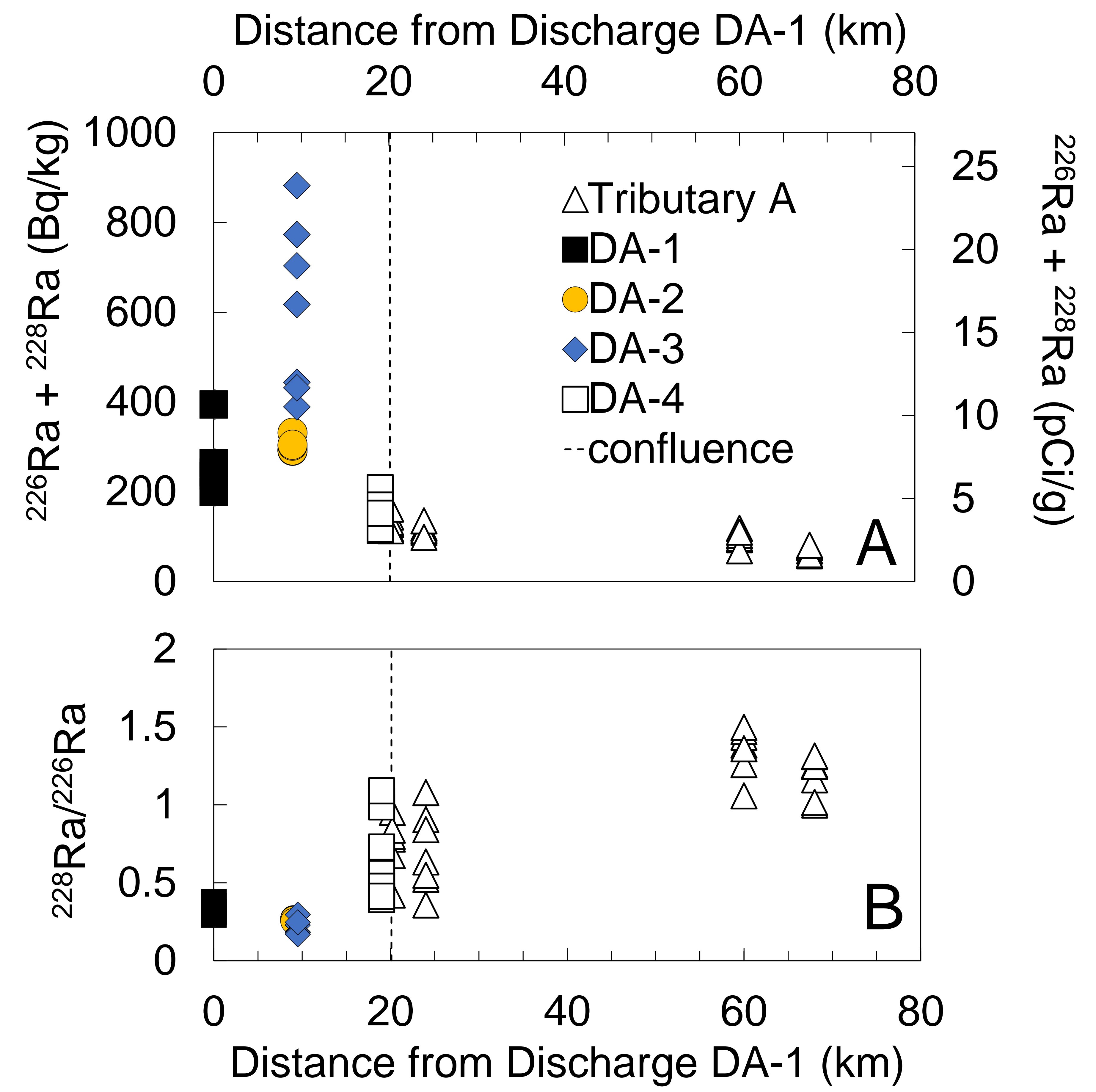
Table 1. Average TDS and radium activities in water and sediment samples \pm standard deviation (SD) collected at each site between 2013-2016. Sites marked with an "x" had average ^{226}Ra activities in sediments more than 185 Bq/kg (5 pCi/g) above background sediments.

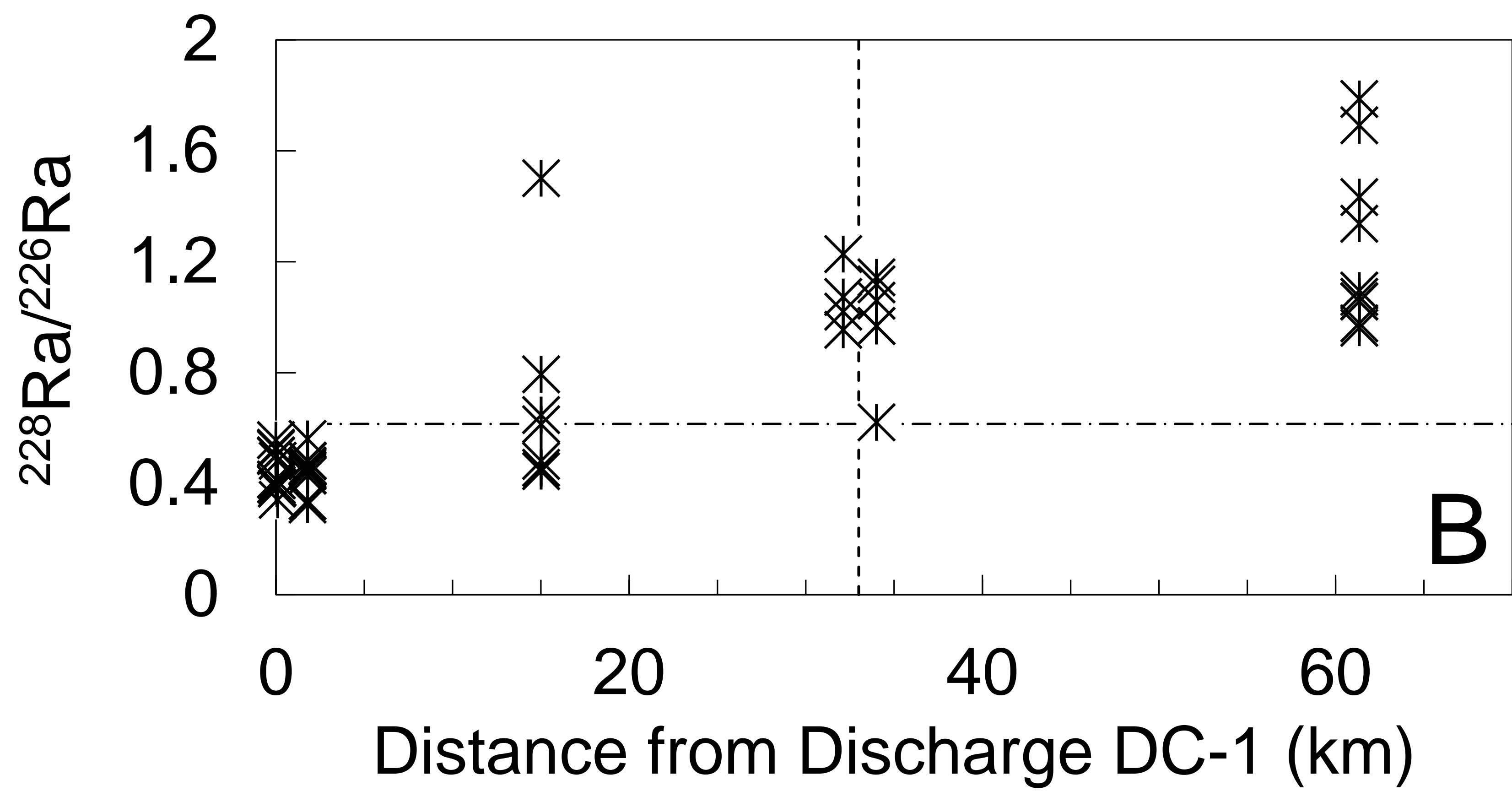
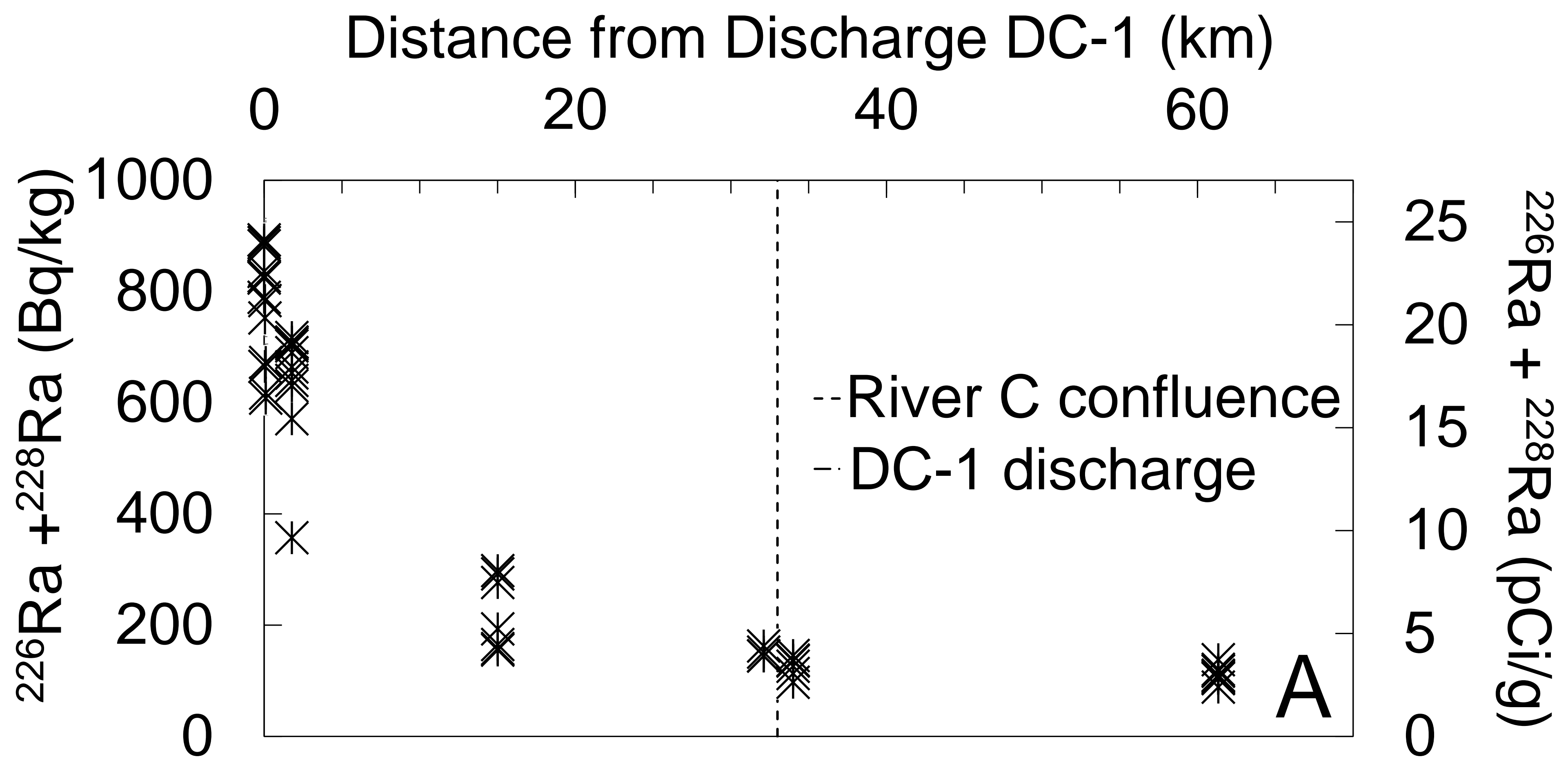
Site Name	TDS (mg/L)	^{226}Ra (pCi/L)	^{226}Ra (Bq/L)	$^{228}\text{Ra}^*$ (pCi/L)	$^{228}\text{Ra}^*$ (Bq/L)	$^{226}\text{Ra}+^{228}\text{Ra}$ (Bq/L)	Dissolved $^{226}\text{Ra}/^{228}\text{Ra}$	^{226}Ra (Bq/kg)	^{228}Ra (Bq/kg)	$^{226}\text{Ra}+^{228}\text{Ra}$ (Bq/kg)	$^{226}\text{Ra}+^{228}\text{Ra}$ (pCi/g)	Sediment $^{226}\text{Ra}/^{228}\text{Ra}$	Fails to meet sediment regulatory limit	# samples dissolved	# samples sediment
A1	1408 \pm 193	1.91 \pm 0.29	0.07 \pm 0.01	2.34	0.09	0.16	1.22	76 \pm 18	57 \pm 9	134	3.6	0.8		11	6
A2	1271 \pm 120	1.29 \pm 0.58	0.05 \pm 0.02	nd	nd	0.05	nd	68 \pm 4	49 \pm 15	117	3.2	0.7		11	7
A3	1621 \pm 209	nd	nd	nd	nd	nd	nd	41 \pm 5	56 \pm 11	97	2.6	1.4		11	7
A4	1730 \pm 303	0.21 \pm 0.10	0.01 \pm 0.00	1.13	0.04	0.05	5.37	31 \pm 4	36 \pm 7	67	1.8	1.2		10	7
DA-1	528 \pm 95	4.98 \pm 0.74	0.18 \pm 0.03	1.31	0.05	0.23	0.26	238 \pm 58	77 \pm 17	315	8.5	0.3	x	11	5
DA-2	1172 \pm 104	4.04 \pm 0.56	0.15 \pm 0.02	1.18	0.04	0.19	0.29	237 \pm 11	63 \pm 3	300	8.1	0.3	x	11	7
DA-3	1234 \pm 235	9.03 \pm 2.66	0.33 \pm 0.10	1.40	0.05	0.39	0.15	483 \pm 173	100 \pm 20	583	15.7	0.2	x	11	7
DA-4	994 \pm 191	0.92 \pm 1.10	0.03 \pm 0.04	2.63	0.10	0.13	2.85	83 \pm 29	57 \pm 7	141	3.8	0.7		10	11
B1	98 \pm 34	0.26 \pm 0.11	0.01 \pm 0.00	nd	nd	0.01	nd	54 \pm 19	362 \pm 308	415	11.2	6.7		8	7
B2	106 \pm 34	0.27 \pm 0.19	0.01 \pm 0.01	nd	nd	0.01	nd	30 \pm 7	67 \pm 19	98	2.6	2.2		8	7
B3	107 \pm 38	0.27 \pm 0.16	0.01 \pm 0.01	1.17	0.04	0.05	4.39	44 \pm 6	137 \pm 18	181	4.9	3.1		10	7
UDB-1.0	446 \pm 179	0.33 \pm 0.10	0.01 \pm 0.00	nd	nd	0.01	nd	40 \pm 3	54 \pm 7	94	2.5	1.3		5	7
DB-1.0	6709 \pm 3052	0.18 \pm 0.10	0.01 \pm 0.00	1.14	0.04	0.05	6.39	55 \pm 6	53 \pm 6	108	2.9	1.0		3	4
DB-1.1	459 \pm 190	0.32 \pm 0.27	0.01 \pm 0.01	1.40	0.05	0.06	4.37	44 \pm 3	78 \pm 10	122	3.3	1.8		8	7
DB-2.0	3822 \pm -	33.40 \pm -	1.24 \pm -	23.80	0.88	2.12	0.71	2690 \pm 130	763 \pm 50	3453	93.3	0.3	x	1	3
DB-2.1	5089 \pm 965	12.95 \pm 2.76	0.48 \pm 0.10	5.85	0.22	0.70	0.45	309 \pm 79	68 \pm 28	378	10.2	0.2	x	2	7
DB-2.2	5264 \pm 1164	8.93 \pm 1.77	0.33 \pm 0.07	2.42	0.09	0.42	0.27	51 \pm 4	89 \pm 20	139	3.8	1.7		7	7
DB-3	754 \pm 333	0.48 \pm 0.14	0.02 \pm 0.01	nd	nd	0.02	nd	53 \pm 2	83 \pm 5	136	3.7	1.6		3	7
DB-4.0	5693 \pm 874	4.56 \pm 1.28	0.17 \pm 0.05	3.30	0.12	0.29	0.72	99 \pm 3	111 \pm 3	210	5.7	1.1		3	4
DB-4.1	1641 \pm 884	0.25 \pm 0.07	0.01 \pm 0.00	1.07	0.04	0.05	4.32	42 \pm 14	83 \pm 28	125	3.4	1.9		10	6
C1	139 \pm 79	0.86 \pm 0.35	0.03 \pm 0.01	nd	nd	0.03	nd	36 \pm 7	35 \pm 5	71	1.9	1.0		13	7
C2	144 \pm 81	0.79 \pm 0.31	0.03 \pm 0.01	nd	nd	0.03	nd	62 \pm 10	64 \pm 13	126	3.4	1.0		13	6
C3	285 \pm 157	0.44 \pm 0.14	0.02 \pm 0.01	nd	nd	0.02	nd	48 \pm 9	63 \pm 10	111	3.0	1.3		11	10
DC-1	1174 \pm 60	7.12 \pm 0.72	0.26 \pm 0.03	4.38	0.16	0.43	0.62	570 \pm 13	279 \pm 35	849	23.0	0.5	x	9	7
DC-2	1175 \pm 163	6.26 \pm 0.69	0.23 \pm 0.03	3.28	0.12	0.35	0.52	436 \pm 65	183 \pm 41	619	16.7	0.4	x	14	12
DC-3	1996 \pm 255	1.15 \pm 0.48	0.04 \pm 0.02	nd	nd	0.04	nd	133 \pm 58	81 \pm 14	214	5.8	0.6		10	7
DC-4	2054 \pm 400	nd	nd	nd	nd	nd	nd	73 \pm 4	78 \pm 7	151	4.1	1.1		3	4
Reference site	1651 \pm 1283	0.47 \pm 0.07	0.02 \pm 0.00	nd	nd	0.02	nd	52 \pm 8	77 \pm 17	129	3.5	1.5		5	7

*Insufficient number of detectable measurements for SD calculation

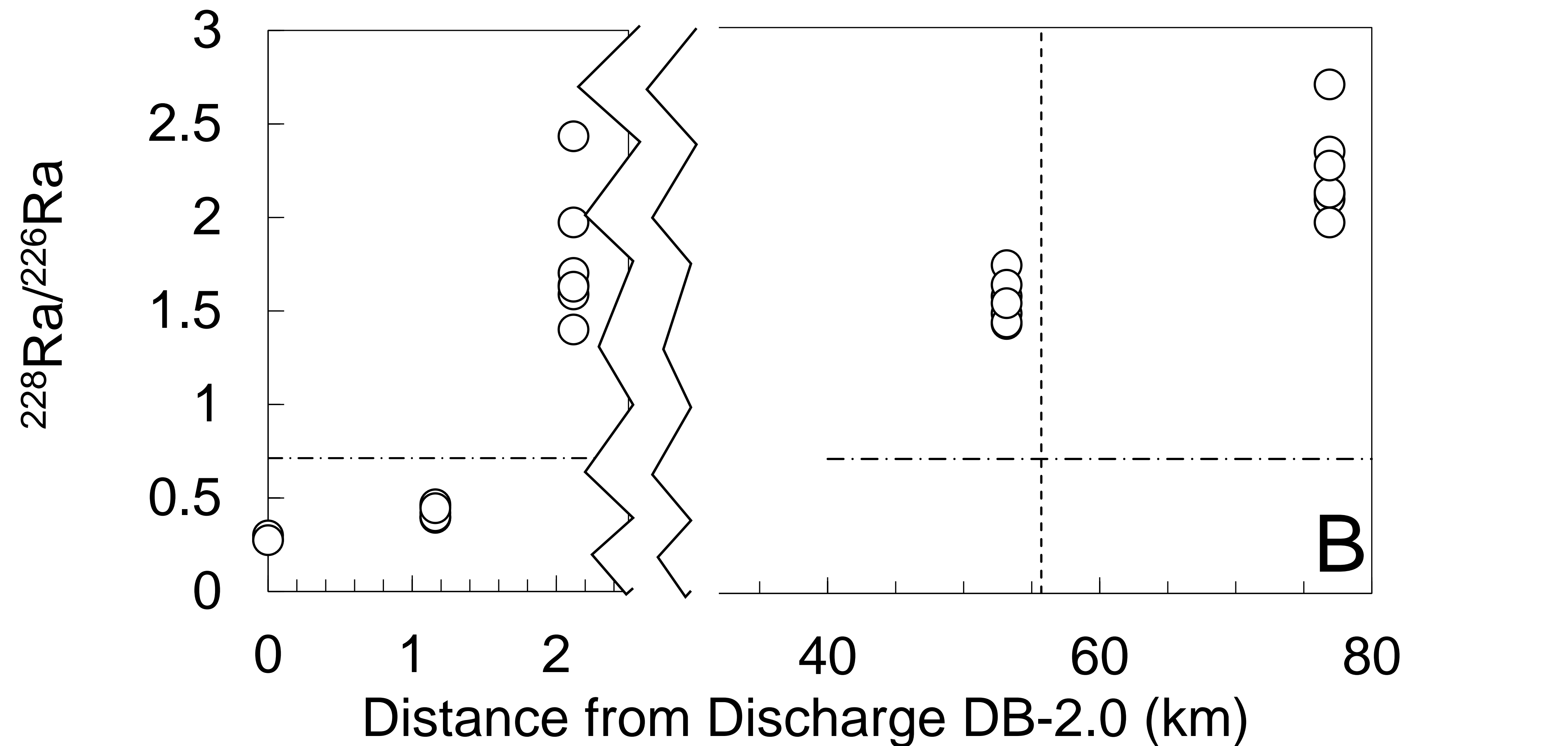
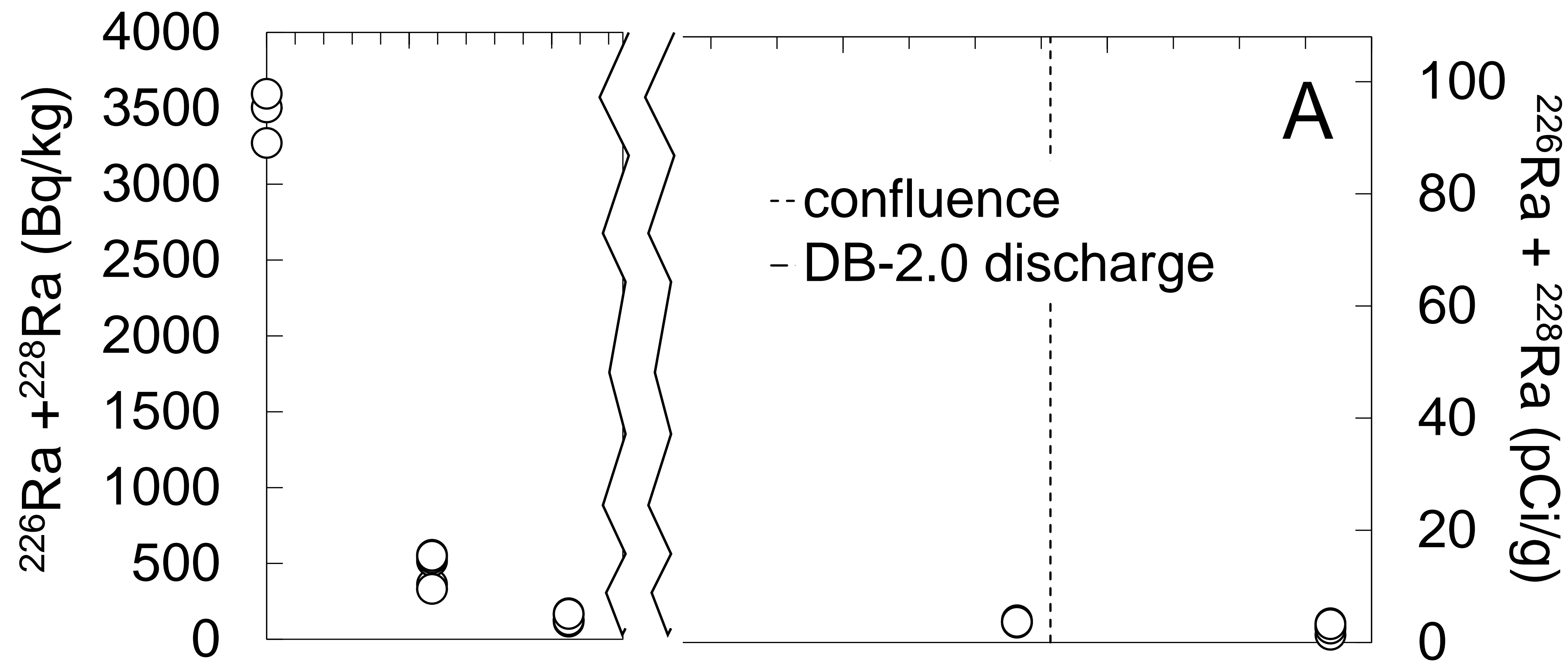


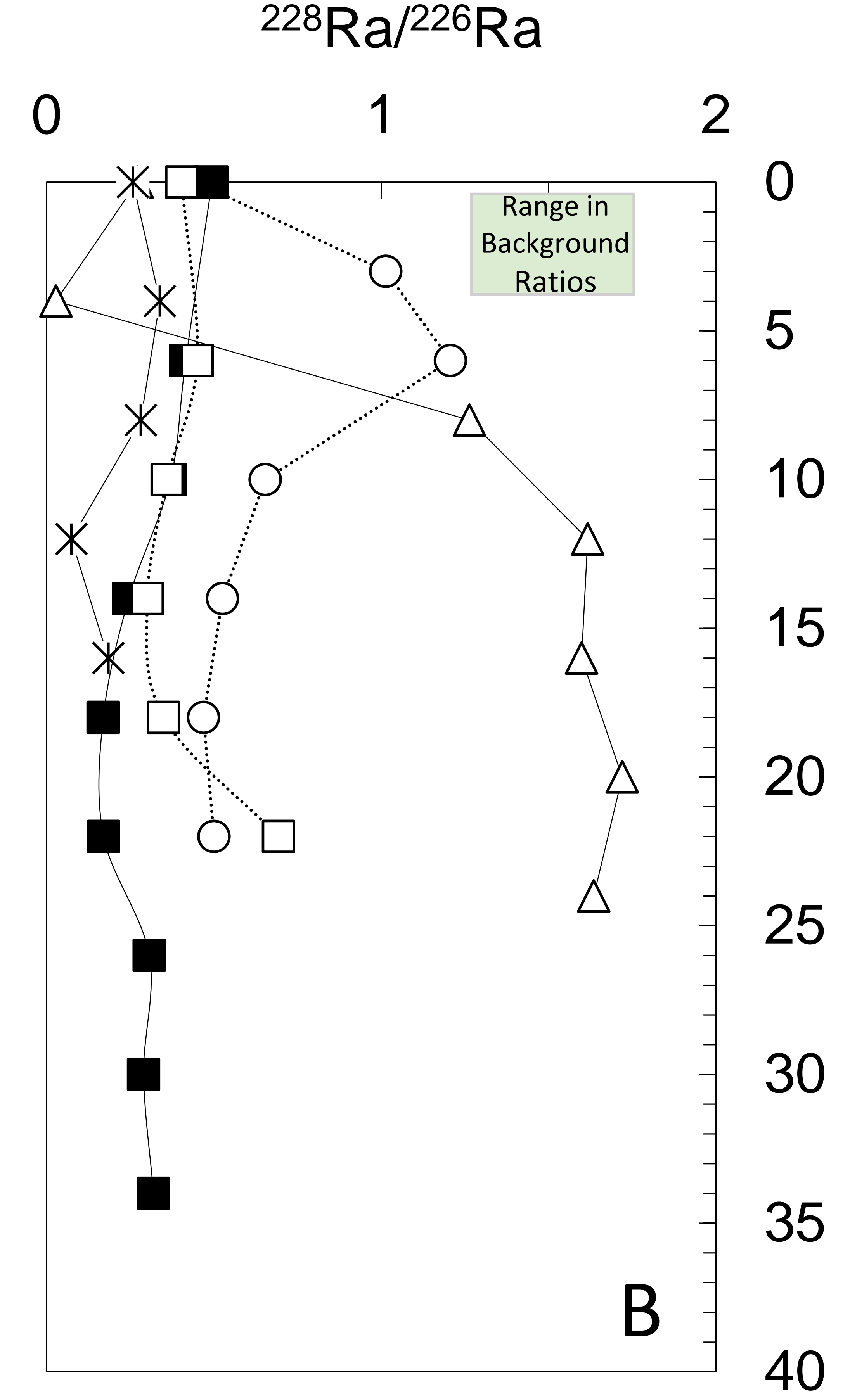
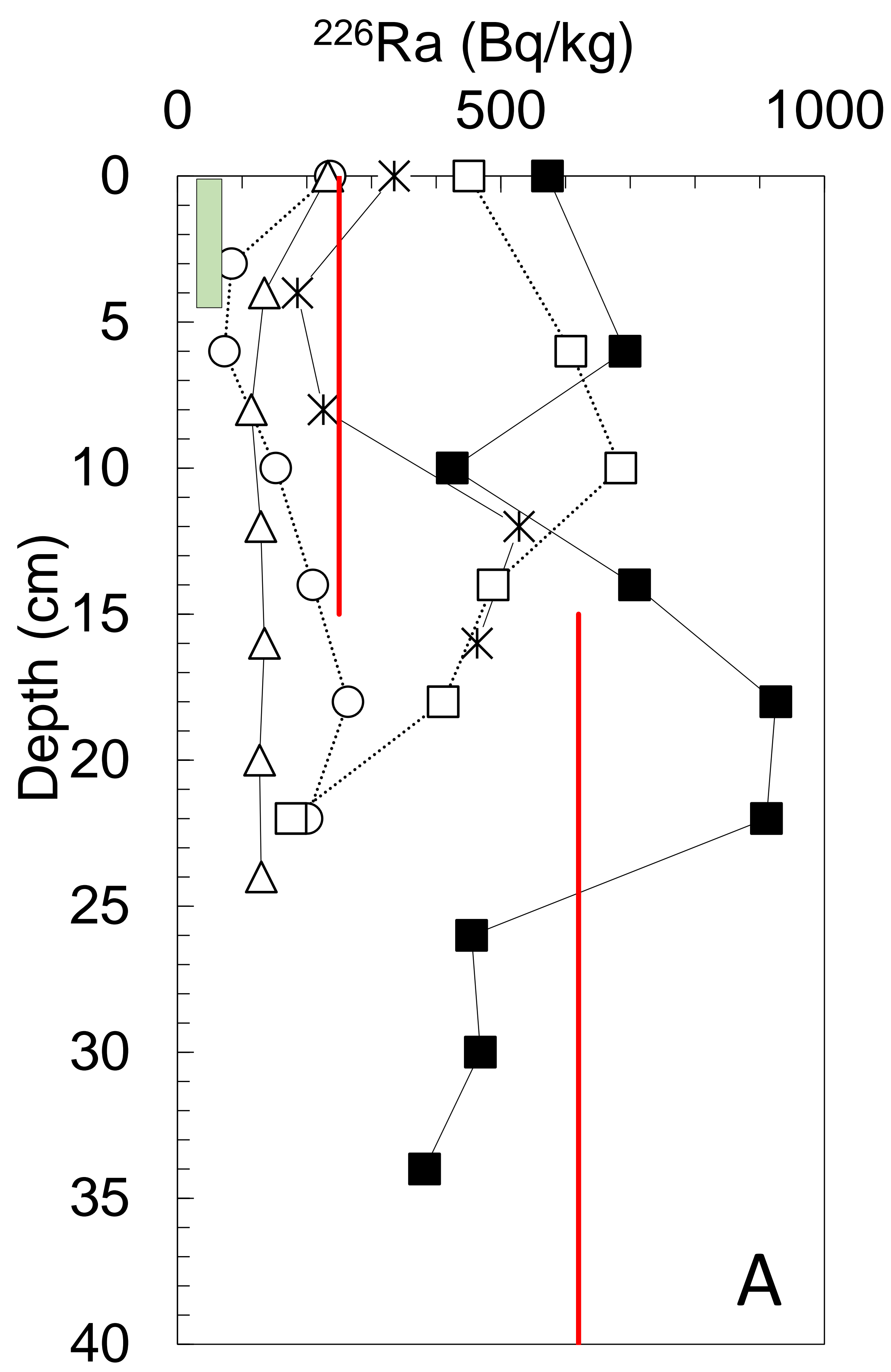
1
2
3
4
5
6
7
8
9
10
11
12
13
14
15
16
17
18
19
20
21
22
23
24
25
26
27
28
29
30
31
32
33
34
35
36
37
38
39
40
41
42
43
44
45
46
47
48
49
50
51
52
53
54
55
56
57
58
59
60





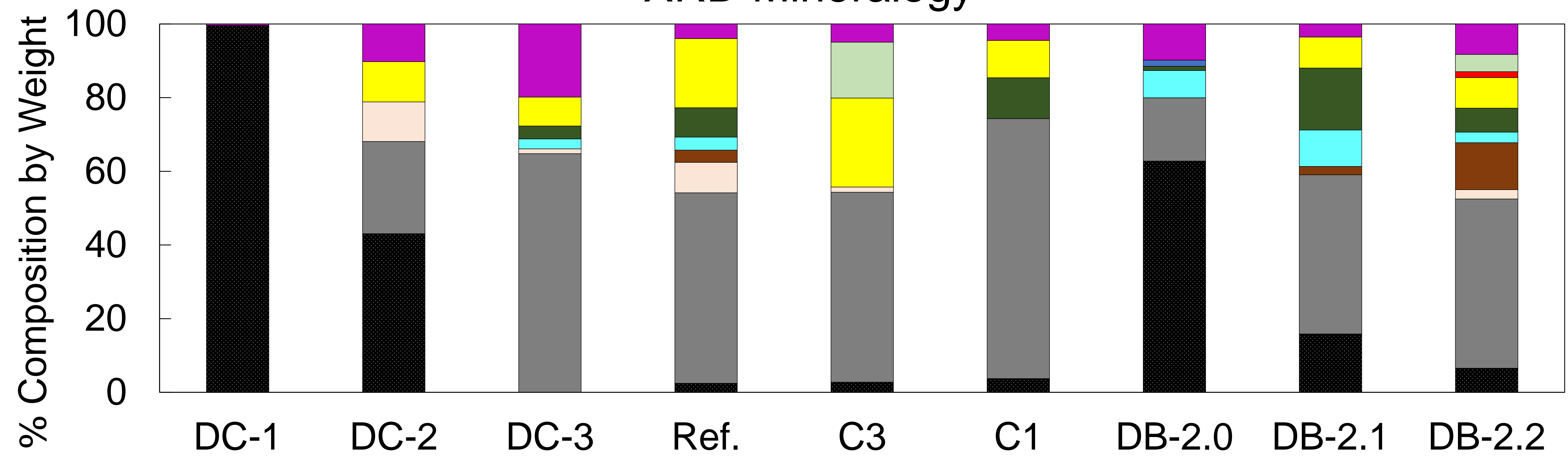
Distance from Discharge DB-2.0 (km)



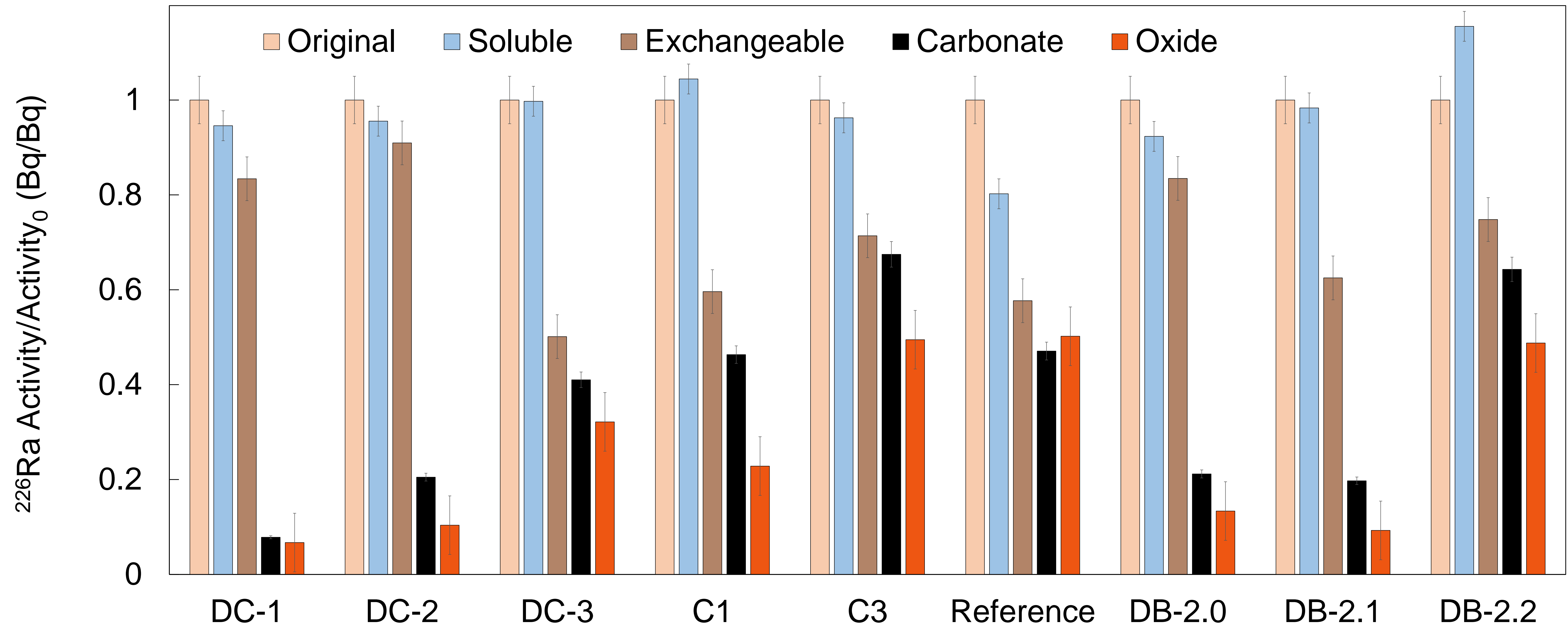


- DB-2.1
- △ DA-2
- * DA-3
- DC-1
- DC-1 100m
- Regulatory Limits

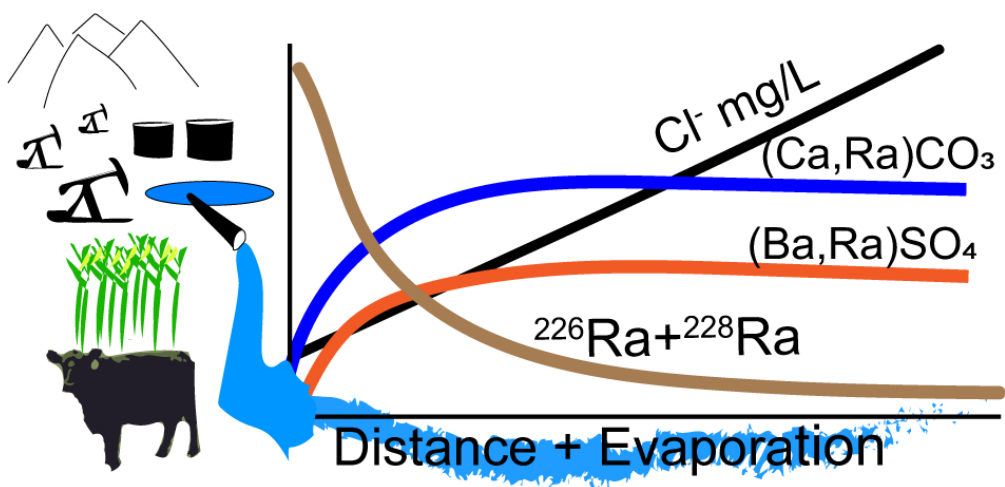
XRD Mineralogy



- CaCO3
- Muscovite
- Dolomite
- Albite
- Kaolinite
- Minerals < 5%
- SiO2
- Illite
- Microcline
- Gypsum
- Tentatively Identified Compounds



1
2
3
4
5
6
7
8
9
10
11
12
13
14
15
16
17
18
19
20
21
22
23
24
25
26
27
28
29
30
31
32
33
34
35
36
37
38
39
40
41
42
43
44
45
46
47
48
49
50
51
52
53
54
55
56
57
58
59
60



80x38mm (300 x 300 DPI)